Pro-resolving mediator protectin D1 promotes epimorphic regeneration by controlling immune cell function in vertebrates

Mai Nguyen-Chi, Patricia Luz-Crawford, Laurence Balas, Tamara Sipka, Rafael Contreras-López, Audrey Barthelaix, Georges Lutfalla, Thierry Durand, Christian Jorgensen, Farida Djouad

RESEARCH PAPER

Pro-resolving mediator protectin D1 promotes epimorphic regeneration by controlling immune cell function in vertebrates

Mai Nguyen-Chi[1,2] | Patricia Luz-Crawford[3] | Laurence Balas[4] | Tamara Sipka[2] | Rafael Contreras-López[1,3] | Audrey Barthelaix[1] | Georges Lutfalla[2] | Thierry Durand[4] | Christian Jorgensen[1] | Farida Djouad[1]

[1]IRMB, INSERM, Univ Montpellier, CHU Montpellier, Montpellier, France

[2]LPHI, CNRS, Univ Montpellier, Montpellier, France

[3]Centro de Investigación Biomédical, Facultad de Medicina, Universidad de los Andes, Santiago, Chile

[4]IBMM, UMR5247, CNRS, Univ Montpellier, ENSCM, Montpellier, France

Correspondence
Mai Nguyen-Chi, LPHI, CNRS, Univ Montpellier, Montpellier, France.
Email: mai-eva.nguyen-chi@umontpellier.fr

Farida Djouad, Inserm U1183, IRMB, 80 avenue Augustin Fliche, Montpellier, France.
Email: farida.djouad@inserm.fr

Funding information
Marie-Curie Innovative Training Network ImageInLife, Grant/Award Number: 721537; INSERM

Background and Purpose: Specialized pro-resolving mediators (SPMs) are a family of lipids controlling the resolution of inflammation and playing a role in many processes including organ protection and tissue repair. While SPMs are potent bioactive molecules *in vivo*, their role in epimorphic regeneration of organs in vertebrates has not been tested. Using the zebrafish larva as a robust regenerative vertebrate system, we studied the role of the SPM neuroprotectin/protectin D1 (PD1) during the caudal fin fold regeneration.

Experimental Approach: Regeneration of the fin fold was analysed when exposed to a synthetic PD1. The effect of PD1 on immune cell recruitment and activation was further investigated using live imaging combined with fluorescent reporter lines. Using genetic and pharmacological approaches, we dissected the role of neutrophils and macrophages on driving the pro-regenerative effect of PD1.

Key Results: We showed that PD1 improves fin fold regeneration. Acting in a narrow time window during regeneration, PD1 accelerates the resolution of inflammation without affecting the initial kinetic of neutrophil recruitment but instead, promotes their reverse migration potential. In addition, PD1 induces macrophage polarization switch towards non-inflammatory states in both zebrafish and mammalian system. Finally, macrophages but not neutrophils are essential for PD1-mediated regeneration.

Conclusion and Implications: These results reveal the pro-regenerative action of PD1 and its role in regulating neutrophil and macrophage response in vertebrates. These findings strongly support the development of pro-resolving mediators as natural therapeutic candidates for degenerative disorders and the use of the zebrafish as a tool to investigate pro-regenerative drugs.

1 | INTRODUCTION

Contrary to mammals, some vertebrates possess the extraordinary capacity to fully replace organs or tissue portions after amputation or injury (Akimenko, Marí-Beffa, Becerra, & Géraudie, 2003; Gemberling, Bailey, Hyde, & Poss, 2013; Kawakami, Fukazawa, & Takeda, 2004; Tal, Franzosa, & Tanguay, 2010). This regeneration process, called epimorphic regeneration, relies on the formation of a highly proliferative

Abbreviations: ccr2, CC Chemokine Receptor 2; ef1a, elongation factor 1-α; Gpr37, G-coupled protein receptor 37; lyz, lysozyme C; mfap4, microfibril associated protein 4; mpeg1, macrophage express gene 1; mpx, myeloperixidase; MTZ, metronidazole; n–3 DPA, n-3 docosapentaenoic acid; NTR, nitroreductase; PD1, protectin D1; rcn3, reticulocalbin 3; rzfTnfa, recombinant zebrafish TNFα; SPM, specialized pro-resolving mediator.

structure named blastema (Alvarado & Tsonis, 2006). Discovering new mechanisms by which regeneration can be therapeutically enhanced in regenerative species is a key step to develop more effective therapies to promote tissue regeneration in mammals. In response to injury, neutrophils and macrophages, key mediators of inflammation, infiltrate the wound and participate in tissue repair (Larouche, Sheoran, Maruyama, & Martino, 2018). Recently, we and others have shown the instrumental role of immune cells and inflammation in epimorphic regeneration and blastema formation in highly regenerative animals. Indeed, in adult axolotls, macrophages are required for limb regeneration after amputation (Godwin, Pinto, & Rosenthal, 2013). The analysis of ear wound regeneration after an injury in the African spiny mouse (*Acomys cahirinus*), a mammalian model of epimorphic regeneration, revealed the important role of immune cells, especially activated macrophage subtypes, in the control of ear regeneration (Simkin, Gawriluk, Gensel, & Seifert, 2017). Similar mechanisms were reported in the adult zebrafish where macrophages are necessary to initiate fin regeneration and control fin patterning (Petrie, Strand, Tsung-Yang, Rabinowitz, & Moon, 2014). More recently, we showed that the caudal fin fold regeneration of the zebrafish larvae depends on tightly regulated macrophage subtype recruitment and activation at the wound site (Nguyen-Chi et al., 2017). Indeed, we demonstrated that pro-inflammatory (M1-like) macrophages, accumulating during the early phase of regeneration, are required for blastema formation, while non-inflammatory (M2-like) macrophages accumulating at later stages of the process, are important for the fin structure. Furthermore, we identified polarized macrophage-derived TNFα as a necessary signal that creates a permissive environment for regeneration (Nguyen-Chi et al., 2017). All these studies emphasize the crucial role of a tightly regulated inflammation response in the regeneration process. While very few molecules promoting regeneration have been identified, therapeutic targeting of inflammatory mediators arises as an attractive approach to enhance regeneration. However, any attempt to manipulate inflammation using chemicals, either by induction of a persistent inflammation or by inhibition of this process, impedes regeneration in highly regenerative species (Hasegawa et al., 2017; Mathew et al., 2007; Miskolci et al., 2019).

In this respect, specialized pro-resolving mediators (SPMs) appear as attractive molecules to control epimorphic regeneration. SPMs encompass separate families of lipids including **lipoxins**, **resolvins**, protectins and maresins that are potent modulators of the resolution phase of inflammation, behaving as agonists (Serhan, 2014; Spite, Clària, & Serhan, 2014). Produced by human and mouse immune cells, all members of SPM families share a capacity to modulate local inflammation, limit the infiltration of polymorphonuclear neutrophils in the injury/infection site while promoting the uptake of apoptotic cells, debris and microbes by macrophages (Serhan, Chiang, & Dalli, 2015). Thus, SPMs are at the forefront of homeostasis regulation. Among the SPMs, neuroprotectin/protectin D1 (NPD1/PD1, here referred as PD1), a dihydroxylated docosatriene derived from **docosahexaenoic acid** (DHA), that is structurally unique from the other SPMs because it possesses a E,E,Z-conjugated triene and also has aroused a growing interest (Hansen, Vik, & Serhan, 2019; Petasis et al., 2012; Serhan et al., 2006) due to its capacity to activate inflammation–resolution programmes at nanomolar concentrations. It is endogenously produced by platelets, macrophages and polymorphonuclear neutrophils in mammals and is also detected in trout's head-kidney, the haematopoietic organ in fish, suggesting a conserved role for PD1 in the immune system from fish to mammals (Hong et al., 2007; Serhan, 2014). Although often confused, PD1 differs from its isomer, protectin DX (PDX) which has been reported to possess lower bioactivity (Balas, Guichardant, Durand, & Lagarde, 2014; Hansen et al., 2019; Serhan et al., 2006). PD1 was reported to accelerate resolution of *Escherichia coli* infection in murine peritonitis by enhancing bacterial uptake and killing by neutrophils (Chiang et al., 2012). In addition, PD1 is able to accelerate healing and nerve-fibre growth of skin wounds of diabetic mice. This protective effect is presumably due to PD1 bio-action on macrophage functions (Hong et al., 2014). Recent studies have shown that PD1 profile changes according to activated macrophage subtypes (Dalli & Serhan, 2017). Similarly, Maresin 1 (macrophage mediators in resolving inflammation 1), a regioisomer of PD1, is produced at higher levels in alternatively activated M2 macrophages than in classically activated M1 (Dalli et al., 2016; Ramon et al., 2016; Xu et al., 2013) and Maresin molecules or precursors promote macrophage polarization towards M2 phenotype in vitro (Dalli, Zhu, et al., 2013). n-3 docosapentaenoic acid-derived protectin ($PD_{n\text{-}3\ DPA}$), a recently discovered member of

What is already known

- Specialized pro-resolving mediator protectin D1 (PD1) is potent modulator of the resolution phase of inflammation.
- PD1 carries potent protective properties and favours tissue repair in different systems.

What this study adds

- Synthetic PD1 improves epimorphic regeneration in vertebrates.
- PD1 modulates leukocyte function and its pro-regenerative effect is dependent on macrophages but not neutrophils.

What is the clinical significance

- Our findings support the potential of PD1 and related molecules as therapeutics for degenerative disorders.
- This study highlights the use of the zebrafish as a tool to investigate pro-regenerative drugs.

the SPM family, regulates the differentiation and activation of human monocytes (Dalli, Colas, & Serhan, 2013; Pistorius et al., 2018). Interestingly, in the non-vertebrate Planaria, a highly regenerative model, maresin has been shown to increase regeneration after injury (Serhan et al., 2012). While SPMs are considered to be putative pro-regenerative molecules, their role in epimorphic regeneration in vertebrate has never been investigated.

Combining transparency and regenerative capacity, the zebrafish larva is emerging as a powerful system to address in vivo potency of small molecules in vertebrates. In the present study, we used the zebrafish larvae to study the effect of the lipid PD1 on epimorphic regeneration. Using caudal fin amputation to trigger subsequent regeneration, we examine the role of PD1 on fin fold regeneration and in controlling inflammation resolution.

2 | METHODS

2.1 | Ethics statement

Animal experimentation procedures were carried out by following the 3Rs, replacement, reduction and refinement, principles according to the European Union guidelines for handling of laboratory animals (http://ec.europa.eu/environment/chemicals/lab_animals/home_en.htm) and were approved by the Comité d'Ethique pour l'Expérimentation Animale under reference CEEA-LR-B4-172-37 and APAFIS#5737-2016061511212601 v3. Animal studies are reported in compliance with the ARRIVE guidelines (Kilkenny, Browne, Cuthill, Emerson, & Altman, 2010) and with the recommendations made by the *British Journal of Pharmacology*.

2.2 | Fish husbandry

Zebrafish larvae were used for this study because of their transparency, regenerative capacity and permeability to small molecules. Zebrafish (*Danio rerio*) maintenance and husbandry were performed at the fish facility of the University of Montpellier as described (Kimmel, Ballard, Kimmel, Ullmann, & Schilling, 1995). Males and females were kept in 3.5-L polycarbonate tank (maximum 22 fish per tank) connected to a recirculating system (Tecniplast), in the following conditions: 4‰ salinity/400 conductivity, temperature of 27.5°C and a 12:12-h light:dark cycle. The fish were fed twice per day. Embryos were collected in petri dishes in a zebrafish medium at 28°C and larvae were fed from Days 5. For experiments, larvae were staged and used from 2 days post-fertilization (dpf) to 6 days post-fertilization. Strains used were golden and AB strains (ZIRC Cat# ZL1, RRID:ZIRC_ZL1) and transgenic lines. *Tg(mpeg1:mCherryF)ump2Tg* (ZFIN Cat# ZDB-GENO-130722-1, RRID:ZFIN_ZDB-GENO-130722-1), referred as *Tg(mpeg1:mCherry-F)* (Nguyen-Chi et al., 2014) and *Tg(mfap4:mCherry-F)ump6Tg*, referred as *Tg(mfap4:mCherry-F)* (Phan et al., 2018), were used to visualize macrophages. *Tg(mpx:eGFP)i114* (Renshaw et al., 2006) (ZFIN Cat# ZDB-GENO-170316-1, RRID:ZFIN_ZDB-GENO-170316-1), referred as *Tg(mpx:eGFP)*, *Tg(mpx:Dendra2)uwm4* (Yoo & Huttenlocher, 2011) (ZFIN Cat# ZDB-ALT-110209-4, RRID:ZFIN_ZDB-ALT-110209-4), referred as *Tg(mpx:Dendra)*, and *Tg(lyz:DsRed)nz50* (Hall, Flores, Storm, Crosier, & Crosier, 2007) (ZFIN Cat# ZDB-GENO-150602-19, RRID:ZFIN_ZDB-GENO-150602-19), referred as *Tg(lyz:DsRed)*, were used to label neutrophils. *Tg(tnfa:GFP-F)ump5Tg* (ZFIN Cat# ZDB-ALT-151130-3, RRID:ZFIN_ZDB-ALT-151130-3) referred as *Tg(tnfa:GFP-F)* were used to visualize cell expressing Tnfa (Nguyen-Chi et al., 2015). *Tg(rcn3:gal4)pd1023Tg (ZFIN Cat# ZDB-ALT-130409-1, RRID:ZFIN_ZDB-ALT-130409-1) and Tg(UAS:mCherry)pd1112Tg (ZFIN Cat# ZDB-ALT-171010-1, RRID:ZFIN_ZDB-ALT-171010-1)* referred as *Tg(rcn3:gal4/UAS:mCherry)* were used to label mesenchymal cells (Ellis, Bagwell, & Bagnat, 2013). *Tg(mpx:Gal4VP16)i222* (Robertson et al., 2014) (ZFIN Cat# ZDB-ALT-160322-6, RRID:ZFIN_ZDB-ALT-160322-6) and *Tg(UAS-E1b:nfsB-mCherry)i149* (Davison et al., 2007) (ZFIN Cat# ZDB-GENO-150206-5, RRID:ZFIN_ZDB-GENO-150206-5), referred as *Tg(mpx:Gal4/UAS:nfsB-mCherry)*, were used to ablate neutrophils. *Tg(mpeg1:Gal4FF)gl25* (Ellett, Pase, Hayman, Andrianopoulos, & Lieschke, 2011) (ZIRC Cat# ZL10336, RRID:ZIRC_ZL10336) and *Tg(UAS-E1b:NfsB-mCherry) i149* referred as *Tg(mpeg1:Gal4/UAS:nfsB-mCherry)* were used to ablate macrophages. Larvae were anaesthetized in embryo medium supplemented with 0.016%Tricaine before any manipulation (amputation or imaging) and if necessary, larvae were incubated in their embryo medium with or without chemicals at 28.5C after manipulation.

2.3 | Protectin D1 (PD1) treatments in zebrafish larvae

PD1 was synthesized as described in Dayaker, Durand and Balas, (2014) and Jónasdóttir et al. (2015). PD1 was dissolved in ethanol as a stock solution at 1 $mg{\cdot}ml^{-1}$. In Figure 1, in Condition 1, different doses, that is, 40, 200 and 400 pg of PD1, were injected in the posterior caudal vein of 3 days post-fertilization larvae, as one shot, 1 h before amputation. Injections of 200 pg of PD1 were used for all other injection experiments. In Condition 2, PD1 was added to the zebrafish medium immediately after amputation at different final concentrations: 20 μM for Figure 1c,f, concentrations of 1, 5, 10 and 20 μM for Figure 1g and 10 μM for all other incubation experiments. PD1 treatment was maintained during the whole course of the experiment except in Figures 1h and S1E. The choice of the method, "injection" versus "incubation," was then determined according to the constrains of the experiments and the number of larvae required for each experiments. For ablation of neutrophils or macrophages experiments, for the analysis of cell proliferation and for live imaging and photoconversion experiments, the method of injection of PD1 was chosen. Untreated and ethanol-treated larvae (0.72% ethanol) were used as controls.

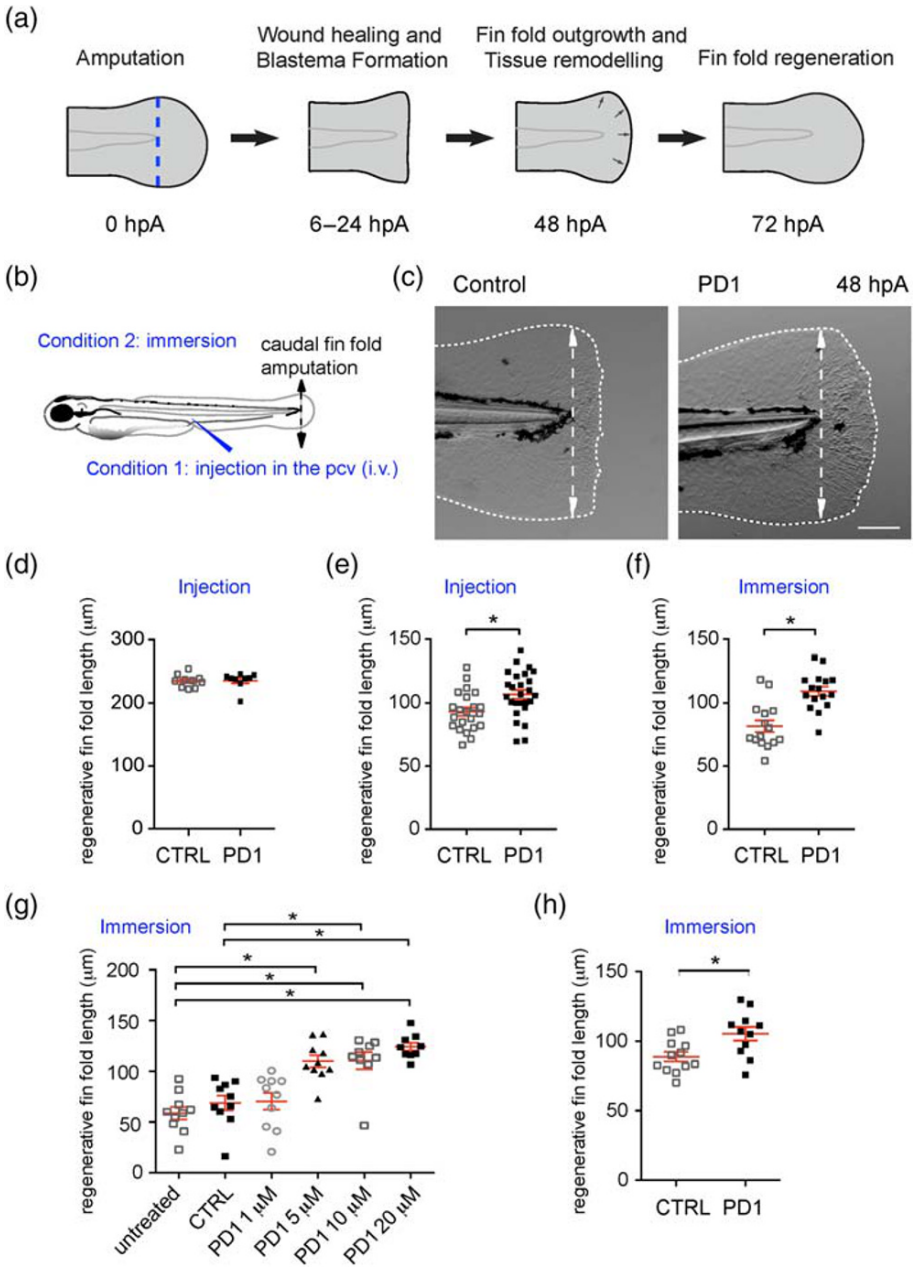

FIGURE 1 PD1 increases regeneration of the caudal fin fold in the zebrafish larvae. (a) Schedule of caudal fin fold regeneration in 3 days post-fertilization (dpf) zebrafish larvae. After fin fold amputation, wound heals and blastema forms within the first 24 h. After 48 h post-amputation (hpA), cell proliferation and mesenchymal cell elongation lead to fin fold outgrowth and tissue remodelling. At 72 hpA, the wound tissue had regrown a regenerative fin fold, achieving the regeneration process. (b) Diagram showing the amputation plane (black arrow) and the two routes of treatments with PD1. In Condition 1, PD1 or ethanol (control; CTRL) was injected in the posterior caudal vein (pcv) (i.v. injection). In Condition 2, PD1 or ethanol (CTRL) was added to the embryo medium (incubation). (c–f) 3 dpf wild-type larvae were treated with either ethanol (CTRL) or PD1 using one of the two conditions and then either kept intact or amputated. (c) Representative transmitted light images of the fin fold at 48 hpA after CTRL and PD1 treatments in the medium (Condition 2). (d) Graph represents the fin fold length at 5 dpA in non-amputated larvae after injection of ethanol (CTRL) or 200-pg PD1 (Condition 1) (mean ± SEM, n_{CTRL} = 10, n_{PD1} = 9, Mann–Whitney test, two-tailed, $P = 0.69$; ns, not significant, representative of two independent experiments). (e) Regenerated fin fold length at 48 hpA in amputated larvae injected with ethanol (CTRL) or 200-pg PD1 (Condition 1) (mean ± SEM, from two independent experiments, n_{CTRL} = 22, n_{PD1} = 26, *t* test, one-tailed, $P < 0.05$). (f) Regenerated fin fold length at 48 hpA in amputated larvae incubated in ethanol (CTRL) or 20-µM PD1 media (Condition 2) (mean ± SEM from two independent experiments, n_{CTRL} = 15, n_{PD1} = 16, Student's *t*-test, one-tailed, $P < 0.05$). (g) Regenerated fin fold length at 48 hpA in amputated larvae incubated in normal medium or media with ethanol (CTRL) or different concentrations of PD1 (Condition 2), (mean ± SEM, n = 9–10, Kruskal–Wallis test with Dunn's multiple comparison as posttest). (h) WT fin folds were amputated at 3 dpf. Ethanol (CTRL) or PD1 (10 µM) was added to the medium for the first 24 h of the regeneration process, then removed. Regenerative fin fold length at 48 hpA in treated larvae (mean ± SEM, n_{CTRL} = 12, n_{PD1} = 11, Student's test, one-tailed, $P < 0.05$, representative of two independent experiments)

2.4 | Larva manipulation for regeneration assays and regeneration quantification

Caudal fin fold amputation was performed in zebrafish larvae as we previously described (Nguyen-Chi et al., 2017). Briefly, larvae were anaesthetized in embryo medium supplemented with 0.016% Tricaine and their fin folds were transected with a scalpel at the limit of notochord posterior end at 3 days post-fertilization. Larvae were replaced in their medium with or without chemicals for 2 or 3 days at 28.5°C. Regenerative fin fold length was calculated as the distance between the amputation plane and the edge of the fin fold in the medial plane. Regenerative fin fold area was calculated as the area of the fin fold from the amputation plane and the edge of the fin fold.

2.5 | Injection of recombinant zebrafish TNFα protein in zebrafish larvae

Wild-type 3 days larvae were anaesthetized in fish water supplemented with 0.016% Tricaine, amputated and injected at 3 h post-amputation (hpA) in the posterior caudal vein with either 1.4 ng of recombinant zebrafish TNFα or PBS-containing elution buffer alone (vehicle) as described in Roca et al. (2008). Effects on regeneration were analysed at 48 hpA.

2.6 | Imaging and neutrophil tracking

For imaging, larvae were anaesthetized in 0.016% Tricaine, immobilized in 35-mm glass-bottom dishes (FluoroDish, World Precision Instruments, UK) using 0.8% low melting point agarose (Sigma-Aldrich, France) and covered with 2 ml of embryo water containing tricaine. Epi-fluorescence microscopy was performed using a MVX10 Olympus microscope (MVPLAPO 1X objective and XC50 camera). Confocal microscopy was performed using an inverted confocal microscope TCSSP5 SP5 (HC PL APO 0.70 20× objective; Leica Microsystems, France). For Acridine Orange staining experiments, images were taken using a ZEISS LSM880 FastAiryscan in a confocal mode. We used a 20×/0.8 Planee apochromat equipped with DIC for transmission images; resolution was chosen at 512 × 512. The wavelengths were respectively 488 nm (Argon Laser) and 561 nm (DSSP Laser) for excitation and we selected 505–550 nm on a PMT detector and 585–620 nm on a GaAsP detector for emission. The images were taken in a sequential mode by line. The 3D files generated by multi-scan acquisitions were processed using Image J. For reverse migrated neutrophil tracking, we photoconverted the Dendra2 protein specifically expressed in neutrophils of *Tg(mpx:Dendra)* embryos raised to 3 days post-fertilization in the dark and injected with 200 pg of PD1 or 5% ethanol i.v., 1 h before caudal fin fold amputation. At 6 h post-amputation, larvae were mounted in 1% low-melting agarose and photoconversion was performed using a 405-nm Laser Cube 405-50C on a confocal TCS SP5 inverted microscope (HC PL APO 0.70 ∞(infinity) 20× objective, Leica) with 12.5% laser power scanning for 23 s (optimized before the experiments; data not shown). The region of interest for photoconversion was selected in the wound region (200 μm). Tails were imaged before and after the photoconversion at 6 h post-amputation and then at 10 h post-amputation using 490- and 553-nm lasers. Time-lapse video microscopy of neutrophil behaviour at the wound was performed using ANDOR CSU-W1 confocal spinning disc on an inverted NIKON microscope (Ti Eclipse) with ANDOR Neo sCMOS camera (20× air/NA 0.75 objective). Image stacks for time-lapse movies were acquired at 28°C every 4 min, typically spanning 100 μm at 4-μm intervals. The 4D files generated from time-lapse acquisitions were processed using Image J (ImageJ, RRID: SCR_003070), compressed into maximum intensity projections and cropped. Brightness, contrast and colour levels were adjusted for maximal visibility. For the measurements of the velocity and the circularity of reverse migrated neutrophils, neutrophils recruited at the wound were analysed using ImageJ using the following workflow: neutrophils were (1) tracked using "manual tracking" plugin and (2) converted to binary images using "make binary" function and measured for circularity ("shape descriptors" tool).

2.7 | Cell quantification and FACS analysis on zebrafish

For quantification of recruited leukocytes, *Tg(mpx:eGFP)* or *Tg(mpeg1:mCherry-F/tnfa:eGFP-F)* larvae were anaesthetized in Tricaine at 3 days post-fertilization, amputated and immediately incubated with PD1 or ethanol (see above). Larvae and fins were imaged repeatedly at indicated time points using MVX10 Olympus microscope. Recruited leukocytes were counted directly on microscopy images. Total numbers of fluorescent neutrophils or macrophages were quantified as Leukocyte Units (LUs) by computation using Fiji (Fiji, RRID:SCR_002285) as following:- (1) leukocytes were detected using "Find Maxima" function, (2) maxima were automatically counted using run ("ROI Manager..."), roiManager("Add") and (3) roiManager("Measure") functions. Alternatively, total population of neutrophils and macrophages were quantified using FACS analysis (LSRFortessa, BD Biosciences, France). Cells from *Tg(mpx:eGFP/mpeg1:mCherry-F)* treated larvae were dissociated as described in Nguyen-Chi et al. (2015) and the frequency of $mCherry^{+}eGFP^{-}$ and $mCherry^{-}eGFP^{+}$ cells was defined using the Flowjo software (Tree start, Ashland, OR, USA) (FlowJo, RRID:SCR_008520).

2.8 | Cell proliferation and neutrophil death quantification

Proliferative cells were labelled using immunodetection with anti-phosphorylated histone 3 antibody (PH3). At 6 and 24 h post-amputation, larvae were fixed in paraformaldehyde 4% overnight at 4°C and stained as described in Nguyen-Chi et al. (2012) using an anti-PH3 antibody (Cell Signaling Technology Cat# 9701, RRID: AB_331535). This Phospho-Histone H3 (Serine 10) polyclonal

antibody was raised in rabbit, diluted at 1/500 in blocking buffer (1% BSA, 1% DMSO, 2% Goat Serum in PBS-1X) and used only one time. As a secondary antibody, we used a Goat anti-Rabbit coupled with Alexa Fluor 488 (Thermo Fisher Scientific Cat# A-11034, RRID:AB_2576217), with a dilution of 1/1,000 in blocking buffer and used only one time. Positive cells were quantified in the fin fold region using fluorescent microscopy and ImageJ software. For quantification of dead neutrophils, *Tg(lyz:DsRed)* larvae were stained using Acridine Orange as previously described in Nguyen-Chi et al. (2017). Acridine Orange positive neutrophils were quantified in the fin fold region using confocal microscopy.

2.9 | Neutrophil and macrophage depletion

For neutrophil depletion, *Tg(mpx:Gal4/UAS:nfsB-mCherry)* embryos, expressing a Nitroreductase-mCherry fusion protein specifically in neutrophils, were placed in fish water containing 10-mM metronidazole (MTZ) supplemented with 0.1% DMSO (MTZ, Sigma-Aldrich) (freshly prepared) at 48 h post-fertilization. Treatment with 0.1% DMSO was used as a control. Effects on neutrophil population and regeneration were analysed at 24, 48 and 72 h post-treatment (hpT). For macrophage depletion, *Tg(mpeg1:Gal4/UAS:nfsB-mCherry)* embryos, expressing a Nitroreductase-mCherry fusion protein specifically in macrophages, were placed in fish water containing 10-mM MTZ supplemented with 0.1% DMSO (MTZ, Sigma-Aldrich) (freshly prepared) at 48 h post-fertilization. Treatment with 0.1% DMSO was used as a control. Effects on macrophage population and regeneration were analysed at 24 and 72 h post-treatment. Alternatively, to induce macrophage depletion, Lipo-Clodronate or Lipo-PBS (clodronateliposomes.com) were injected i.v. in larvae 3 times 3 nl at 2 days post-fertilization. *Tg(mfap4:mCherry-F/*mpx:eGFP) were analysed for depletion and regeneration at 24 and 72 h post-treatment.

2.10 | Isolation and differentiation of mouse macrophages

Macrophages were isolated from bone marrow of C57BL/6 mice (MGI Cat# 5658021, RRID:MGI:5658021). Briefly, bone marrow cells were collected by flushing femurs and tibia and suspended in IMDM media (Gibco, France) supplemented with 10% heat-inactivated qualified FBS (Gibco), penicillin and streptomycin (Gibco), non-essential amino acids, glutamine, sodium pyruvate and β-mercaptoethanol (Gibco) (MLR media) and cultured at 37°C 5% CO_2 for 3 h. The supernatant was then collected and cells plated at a density of 2×10^5 cells·cm^2 in MLR medium containing 20 ng·ml^{-1} of macrophage colony-stimulating factor (M-CSF, R&D System, France). After 5 days of culture, when indicated, macrophages were stimulated using 100 ng·ml^{-1} of LPS with or without PD1 at 200 pM, 2 nM, 20 nM, 200 nM, 2 μM or 20 μM for another 24-h period. Supernatants were then collected for ELISA analysis and the phenotype of the macrophages was evaluated according to the expression of activation molecules such as MHC class II and CD80 by FACS analysis using the LSRFortessa (BD Biosciences, France) and data analysed using the Flowjo software (Tree start, Ashland, OR, USA).

2.11 | RNA preparation on larva tails and quantitative RT-PCR

To determine the relative expression of *tnfb*, *il1b*, *mpeg1*, *tgfb1* and ccr2, total RNA from larva tails (pools of 10 or 12 tails each) was prepared at 17 hpA. RNA preparation and reverse transcription were as described in Nguyen-Chi et al. (2017). Q-RT-PCR analyses were performed using LC480 software. The primers used were the following: ztnfb.fw (5′CGAAGAAGGTCAGAAACCCA 3′), ztnfb.rv (5′GTTGGAATGCCTGATCCACA 3′), zil1b.fw (5′TGGACTTCGCAGCACAAAATG 3′), zil1b.rv (5′GTTCACTTCACGCTCTTGGATG 3′), zmpeg1.fw (5′GTGAAAGAGGGTTCTGTTACA 3′), zmpeg1.rv (5′GCCGTAATCAAGTACGAGTT 3′), zef1a.5 (5′TTCTGTTACCTGGCAAAGGG 3′), zef1a.3 (5′TTCAGTTTGTCCAACACCCA 3′). ztgfb1a.fw (5′CAACCGCTGGCTCTCATTTGA 3′), ztgfb1a.rv (5′ACAGTCGCAGTATAACCTCAGCT 3′), zccr2.fw (5′TGGCAACGCAAAGGCTTTCAGTGA 3′), and zccr2.rv (5′TCAGCTAGGGCTAGGTTGAAGAG 3′).

2.12 | Data and analysis

Studies were designed to generate experimental groups of approximatively equal size. The approximative equal size of the groups is explained by the delicate process of mounting and of manipulation of small and living zebrafish larvae ,which may occasionally lead to the loss of one larva, preventing thus the acquisition of data on this larva and modifying the size of the experimental group. Studies were designed using randomization and blinded analysis, except for MTZ treatment, as MTZ induced a slight curvature of the tip of the tail which prevent blinded analysis. Statistical analysis was undertaken only for studies where each group size was at least $n = 5$. No inclusion of any data of $n < 5$ was made in the manuscript, excepted in Figure 5. In Figure 5, the measured values were highly reproducible; group size was therefore estimated at $n = 4$. The sample size estimation and the power of the statistical test were computed using GPower. A preliminary analysis was used to determine the necessary sample size n of a test given $\alpha < 0.05$ and power (1- β) > 0.80 (where α is the probability of incorrectly rejecting H_0 when is in fact true and β is the probability of incorrectly retaining H_0 when it is in fact false). Then the effect size was determined. Groups include the number of independent values and statistical analysis was done using these independent values. The number of independent experiments (biological replicates) is indicated in the figure legends when applicable. The level of probability

$P < 0.05$ constitutes the threshold for statistical significance for determining whether groups differ and this P value is not varied throughout the results. Graph Pad Prism 7 Software (San Diego, CA, USA) (GraphPad Prism, RRID:SCR_002798) was used to construct graphs and analyse data in all figures. Specific statistical tests were used to evaluate the significance of differences between groups. Mann–Whitney test one-tailed and two-tailed, Student's t test one-tailed and two tailed, Kruskal–Wallis test, ANOVA with Tukey's post-hoc test and Fisher exact test were used and the type of test and P value are indicated in the figure legend. In multigroup studies with parametric variables, post-hoc tests were conducted only if F in ANOVA achieved $P < 0.05$ and there was no significant variance inhomogeneity. No approaches were used to reduce unwanted sources of variation by data normalization or to generate normal (Gaussian) data. No data transformation was performed, so the units of a variable are the units measured. Outliers (maximum, one per group) were excluded in data analysis and presentation of Figures 2b and S1D, and outliers were determined using Grubbs' test (free calculator on GraphPad site https://www.graphpad.com). No Western blotting has been performed. The immuno-related procedures used comply with the recommendations made by the *British Journal of Pharmacology* (Alexander et al., 2018). The data and statistical analysis comply with the recommendations of the *British Journal of Pharmacology* on experimental design and analysis in pharmacology (Curtis et al., 2018).

2.13 | Data sharing statement

Datasets are being deposited on Zenodo (ZENODO, RRID: SCR_004129) and will be available at publication.

2.14 | Nomenclature of targets and ligands

Key protein targets and ligands in this article are hyperlinked to corresponding entries in http://www.guidetopharmacology.org, the common portal for data from the IUPHAR/BPS Guide to PHARMACOLOGY (Harding et al., 2018), and are permanently archived in the Concise Guide to PHARMACOLOGY 2019/20 (Alexander et al., 2019).

3 | RESULTS

3.1 | PD1 enhances regeneration of the caudal fin fold in zebrafish

To investigate the role of SPMs on epimorphic regeneration in vertebrates, we monitored the effect of a synthetic protectin D1 (PD1) (Balas & Durand, 2016; Dayaker et al., 2014; Jónasdóttir et al., 2015) on caudal fin fold regeneration in the 3 days post-fertilization larvae (Figure 1a). Immediately after amputation of the fin fold, PD1 was administered to the larva using two different routes, by injection of 200 pg in the posterior caudal vein (Condition 1, Figure 1b) or by incubation in the larva medium (Condition 2, Figure 1b,c) at 20 μM. We observed that PD1 treatment did not modify the growth of intact fin folds (Figure 1d) and did not induce toxicity. Moreover, it did not affect the early phase of regeneration at 24 h post-amputation nor the size and morphology of the terminally regenerated fin at 72 h post-amputation (Figure S1A,B). By contrast, both PD1 injection and incubation (Conditions 1 and 2) increased the regenerative fin fold growth, as measured as length or/and area from the initial amputation position to the new distal fin fold edge at 48 hpA (Figures 1c,e,f and S1C). Using increasing concentrations of PD1 in the larva medium, we showed that PD1 effect on fin fold regeneration is dose dependent and efficiently enhanced fin fold growth at 48 hpA between 5 and 20 μM (Figure 1g). Thus, further experiments using PD1 by incubation were performed at 10 μM. Similarly, PD1 enhances the regeneration in a dose-dependent manner when different quantities of PD1 (200 and 400 pg) were injected in the vein (Figure S1D). To determine at which stage of the regeneration process PD1 is active, amputated larvae were treated with PD1 only for the first 24 h following amputation. We observed that such PD1 treatment substantially improved caudal fin fold regeneration at 48 hpA compared to control (Figures 1h and S1E).

Fin fold regeneration is characterised by the proliferation of blastema cell in the region next to the stump as soon as 6 h after wounding (Mateus et al., 2012). To test whether PD1-mediated regeneration is correlated to an enhanced cell proliferation at the wound, we quantified phosphorylated histone 3 positive cells ($PH3^+$) at 6 and 24 h post-amputation using immunodetection. While cells proliferated similarly in controls and PD1-treated fin folds in absence of amputation (Figure 2a), cell proliferation was increased at the wound of PD1-treated fin folds compared to control (Figure 2b), suggesting that PD1 triggers blastemal cell proliferation enhancing this regeneration. To assess whether PD1-treated zebrafish larvae regenerate their fin folds properly, we analysed their structures at the cellular level. Mesenchymal cells, one of the main constituents of the larva fin fold, modify their shapes at the wound site during the regeneration process, and from 48 h post-amputation, they start to elongate and recover their initial shape at 72 h post-amputation (Mateus et al., 2012). We thus analysed mesenchymal cell pattern in amputated fins by imaging *Tg(rcn3:gal4/UAS:DsRed)*, a zebrafish reporter line to study mesenchymal cells. At 48 h post-amputation, while mesenchymal cells appeared round and disorganized at the wound site of control fin folds, they harboured an elongated shape in PD1-treated fin folds, just like non-injured fin folds (Figure 2c), showing that PD1 accelerates the recovery of mesenchymal cell shape. Altogether these data show that PD1 accelerates regeneration of the zebrafish fin fold promoting the proliferation of blastemal cells and the restoration of their morphology. This pro-regenerative activity of PD1 can occur at low concentrations, *in vivo*, in vertebrates and is efficient in a narrow window, during the first 24 h of the regeneration process.

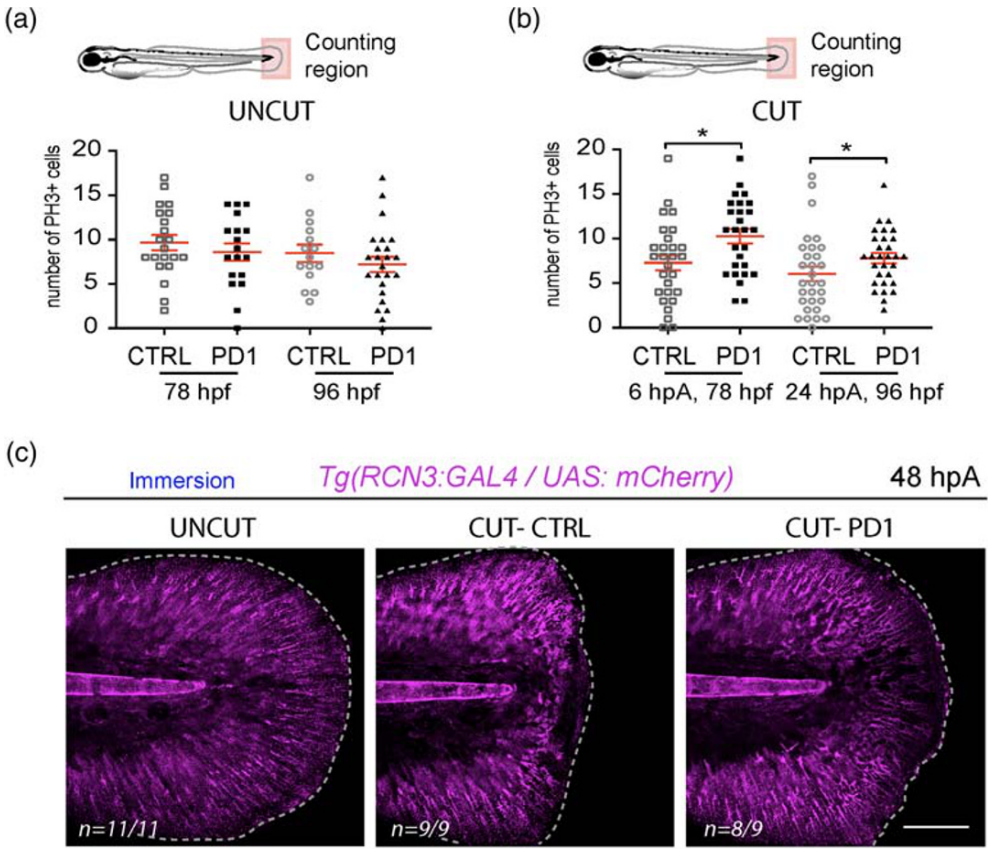

FIGURE 2 PD1 increases cell proliferation and accelerates the recovery of mesenchymal cell morphology at the wound. (a,b) Larvae were injected with ethanol (control; CTRL) or 200-pg PD1 and either kept intact (a) or amputated (b) at 3 days post-fertilization (dpf). Blastema cell proliferation at 6 and 24 h post-amputation (hpA) in indicated conditions was detected using an anti-PH3 antibody ($n_{CTRL/6hpA}$ = 21, $n_{CTRL/24hpA}$ = 15, $n_{PD1/6hpA}$ = 18 and $n_{PD1/24hpA}$ = 24 for uncut/$n_{CTRL/6hpA}$ = 28, $n_{CTRL/24hpA}$ = 30, $n_{PD1/6hpA}$ = 27 and $n_{PD1/24hpA}$ = 30 for cut, mean ± SEM, two independent experiments, Student's t test, two-tailed, *P < 0.05). Larva diagrams represent the regions of counting. (c) *Tg(rcn3:GAL4/UAS:mCherry)* larvae were either kept intact (UNCUT) or amputated (CUT) and incubated with ethanol (CTRL) or PD1 (10 μM). Fin fold images are representative confocal maximum projections of mCherry fluorescence at 48 hpA (n = number of larvae displaying similar phenotype). Scale bar: 100 μm. Dotted lines outline the fin fold

3.2 | PD1 accelerates the resolution of inflammation by promoting neutrophil reverse migration

Immediately after injury, immune cells infiltrate the wound to organize immune defence and promote healing and regeneration (Mescher, Neff, & King, 2017). Since PD1 exerts a beneficial effect on regeneration when added during the first 24 h of the process, we further addressed its function on early regenerative events that involve the immune response. First, the effect of PD1 on the development and recruitment of neutrophils to the wound was addressed using the zebrafish reporter line *Tg(mpx:eGFP)* to track neutrophils. To quantify the total number of neutrophils, 3 days post-fertilization *Tg(mpx:eGFP)* larvae were treated with PD1 or ethanol in the medium and analysed by fluorescent microscopy at 0, 3, 6, and 24 hpT. The total number of neutrophils was not significantly affected after PD1 treatment compared to control (Figures 3a and S2). Similarly, flow cytometry analysis on cells dissociated from the entire *Tg(mpx:eGFP)* larvae, at 6 hpT, confirmed this result (Figure 3b). In parallel, to evaluate the recruitment of neutrophils at the wound site, *Tg(mpx:eGFP)* larvae were amputated at 3 days post-fertilization, incubated in PD1 or ethanol (control), and imaged at different time points after amputation. While the initial recruitment of neutrophils was unchanged by PD1 treatment at 3 and 6 hpA, neutrophil number was significantly decreased at 24 and 48 hpA (Figure 3c,d). We used parameters of neutrophil recruitment at the wound to characterize the resolution phase of inflammation during fin regeneration, as previously described in other contexts (Bannenberg et al., 2005; Lastrucci et al., 2015). The maximum neutrophil number (Ψ_{max}) in control condition was 17.35 at 6 h post-amputation (T_{max}) and it decreased by 50% (Ψ_{50}) at 56 hpA (Table 1). The index of resolution (Ri), which corresponds to the time the neutrophil number decreased by 50% (Ψ_{max}–Ψ_{50}), was therefore 50 h. By contrast, after PD1 treatment, the Ri was 18 h, showing that PD1 is a potent accelerator of inflammation resolution (Table 1). To further investigate by which mechanisms neutrophilic inflammation resolved, we tested whether neutrophil survival was modified by PD1 treatment between 6 and 24 hpA. Using acridine orange staining on neutrophil reporter line, *Tg(lyz:DsRed)*, we detected a very low occurrence of dead neutrophils at the wound in both control and PD1 conditions

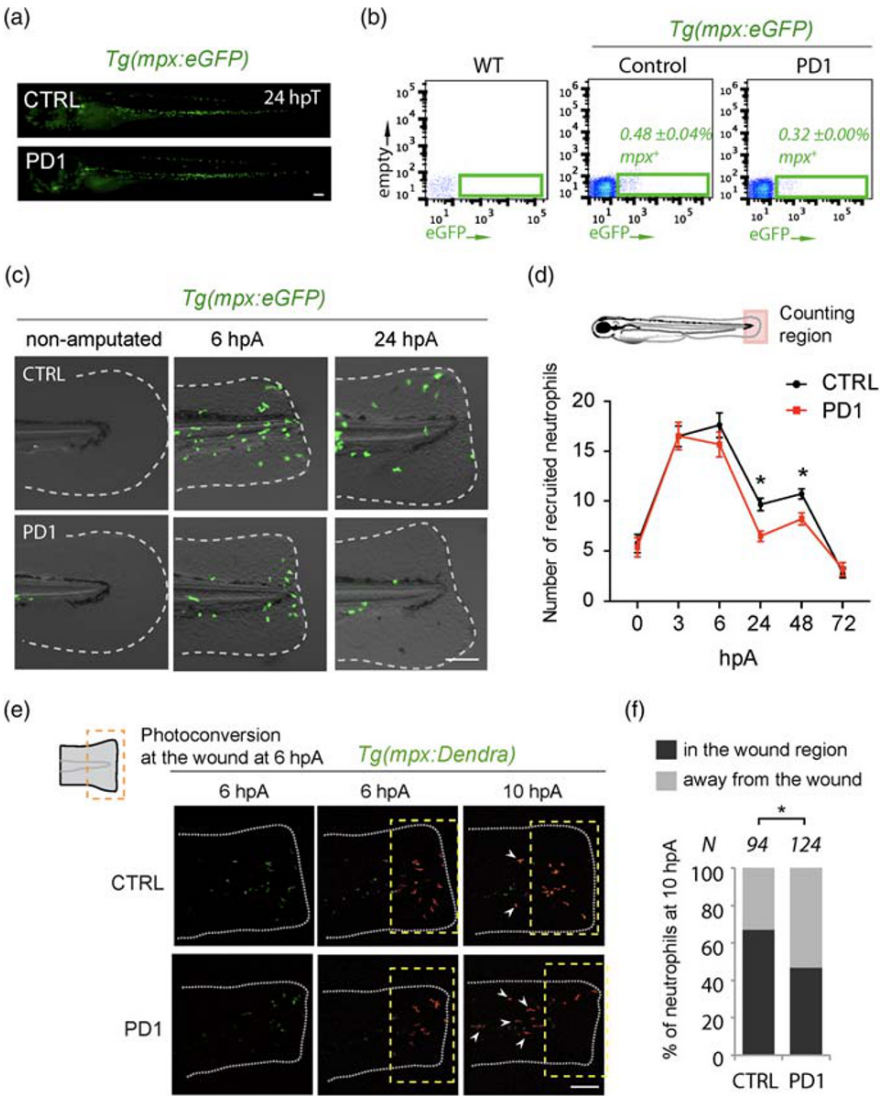

FIGURE 3 PD1 accelerates resolution of inflammation *in vivo* by promoting neutrophil reverse migration. (a) *Tg(mpx:eGFP)* larvae were incubated in ethanol or in 10 μM of PD1 at 3 days post-fertilization (dpf) and GFP fluorescence was analysed by microscopy at 0, 3, 6 and 24 hours post-treatment (hpT). Representative images of neutrophils (GFP) in whole larvae at 24 hpT. (b) Plots represent quantification of neutrophil steady state in WT and in *Tg(mpx:eGFP)* larvae 6 hpT with ethanol (control; CTRL) or PD1 using fluorescence-activated flow cytometry analysis of mpx^+ cells. Cells from a pool of 20 larvae were collected. Gates represent $eGFP^+$ population (the percentage among total cells is indicated) (representative of three experiments). (c) Caudal fin folds of *Tg(mpx:eGFP)* were either kept intact or amputated at 3 dpf and embryos were then incubated in ethanol or PD1 (10 μM). GFP fluorescence was analysed by microscopy at 6 and 24 h post-amputation (hpA). Fin images are representative GFP fluorescence overlaid with transmitted light image. Dotted lines outline the fin fold. (d) Quantification of mpx^+ cells that were recruited in the fin folds at indicated time points following amputation in CTRL or PD1 incubated larvae (mean ± SEM, N = 24–27 per condition, representative of two independent experiments, Mann–Whitney test, one-tailed, $P < 0.05$, CTRL vs. PD1). The diagram shows the region of counting. (e) *Tg(mpx:Dendra)* larvae were injected with ethanol or PD1 (200 pg) and their caudal fin fold was amputated at 3 dpf. Recruited $Dendra^+$ neutrophils (green) were photo-converted to red fluorescence using UV light in the wound region at 6 hpA (dashed boxes). At 10 hpA, the localization of photo-converted neutrophils (red) was analysed by confocal microscopy. Fin fold images are representative maximum projections of confocal fluorescence channels (bottom panels) and overlay with transmitted light image (top panels) before and after photoconversion and 4 h post-photoconversion. Arrowheads indicate photo-converted neutrophils that moved proximally to the wound at 10 hpA. (f) The graph represents the percentage of photo-converted neutrophils that remained in the wound region (dark grey bars) and the percentage of photo-converted neutrophils that migrated away from the wound at 10 hpA (light grey bars). N indicates the total number of neutrophils analysed in the control and PD1-treated conditions (nine to 10 larvae were analysed in each conditions. Fisher's Exact test, $^*P < 0.05$, from two independent experiments). In (a), (c) and (e) scale bar: 100 μm

(Figure S3). Video microscopy of the fin fold from 5 to 13 h post-amputation confirmed that neutrophil survival was not affected by PD1 treatment (Video S1). In addition, the velocity and shape factor (circularity) of neutrophil from PD1-treated wounds were similar from that of controls (Figure S4). As neither the steady state of neutrophils nor their survival were affected by PD1, we hypothesized that

TABLE 1 Indices of resolution of the neutrophil population in the wound region after ethanol (control; CTRL) or protectin D1 (PD1) treatments

	Ψ_{max}	Ψ_{50}	T_{max} (h)	T_{50} (h)	Ri (h)
CTRL	17.35	8.67	6	56	50
PD1	16.23	8.11	3	21	18

Note: These indices were calculated from the kinetics presented in Figure 3d. T_{max} corresponds to the time of maximum neutrophil recruitment (ψ_{max}) and the Resolution index (Ri) to the time for for neutrophils number to decrease by 50% (T_{max}–T_{50}). n = 24–27 larvae per time points.

neutrophilic inflammation resolved through another mechanism than neutrophil death. Reverse migration of neutrophils is a retrograde movement that drives neutrophils away from the site of inflammation. Initially described in response to tail injury in the zebrafish, this phenomenon has been later reported in mammals (Elks et al., 2011; Mathias et al., 2006; Nourshargh, Renshaw, & Imhof, 2016; Tharp et al., 2006). To test the effect of PD1 on reverse migration, we traced neutrophils between 6 and 10 h post-amputation using the *Tg(mpx:Dendra)* line in which neutrophils express the photoconvertible protein Dendra2. At 6 h post-amputation, neutrophils recruited at the wound were photoconverted from green to red fluorescence using UV laser (dashed boxed region) and then imaged 4 h later (10 hpA, Figure 3e). While only 33% of photoconverted neutrophils migrate away from the wound at 10 h post-amputation in the control, 53% of photoconverted neutrophils migrated away from the wound upon PD1 treatment (Figure 3f). Altogether, these data reveal that PD1 accelerates inflammation resolution not by limiting neutrophil infiltration as it was reported in mammals but unexpectedly by enhancing neutrophil reverse migration.

3.3 | PD1 induces macrophage skewing towards a non-inflammatory phenotype in zebrafish

While a number of lines of evidence points out the role of macrophage subsets during appendage regeneration (Godwin et al., 2013; Nguyen-Chi et al., 2017; Petrie et al., 2014), PD1 has been shown to modulate macrophage functions in mouse diabetic wounds (Hong et al., 2014). Thus, to determine the role of PD1 on macrophage steady state, recruitment and activation in our system, we first quantify the total number of macrophages using a zebrafish *Tg(mpeg1:mCherry-F)* reporter line. 3 days post-fertilization *Tg(mpeg1:mCherry-F)* amputated larvae were treated with PD1 or ethanol in the medium and analysed by fluorescent microscopy at 0, 6 and 24 h post-treatment. The total number of macrophages was not significantly affected after PD1 treatment compared to control (Figures 4a and S5). Similarly, flow cytometry analysis on cells dissociated from the entire *Tg(mpeg1:mCherry-F)* larvae, at 6 h post-treatment, confirmed this result (Figure 4b). Then, we analysed the kinetic of macrophage subset recruitment after caudal fin amputation. To specifically track macrophage subsets, we used *Tg(mpeg1:mCherry-F/tnfa:eGFP-F)*, a reporter line that express a farnesylated mCherry (mCherry-F) in all macrophages and both mCherry-F and farnesylated eGFP (GFP-F) in M1-like macrophages expressing *tnfa* (Nguyen-Chi et al., 2015). 3 days post-fertilization *Tg(mpeg1:mCherry-F/tnfa:eGFP-F)* amputated larvae were incubated with PD1 and imaged at different time points following amputation. While the number of macrophages recruited at the wound site at 6 h post-amputation was not significantly affected by PD1 treatment, the number of macrophages at the wound was slightly decreased at 18 and 24 hpA as compared to controls (Figure 4a–c). In addition, upon PD1 treatment, although we did not observe any difference in the number of tnfa$^+$ macrophages recruited at 6 h post-amputation as compared to controls, their number was significantly reduced at 18 and 24 h post-amputation (Figure 4d,e). These data suggest that macrophages switch their phenotypes earlier. To test whether other macrophage subset markers were modified by PD1 treatment, we analysed the expression profile of selected markers at 17 h post-amputation. RNAs were extracted from tails previously treated with CTRL or PD1 and analysed by qRT-PCR (Figure S6A). We showed that PD1 reduced the expression of another M1-like marker, *tnfb*, while the expression of *il1b* and *mpeg1* was not affected (Figure S6B–D). By contrast, PD1 increased *tgfb1a* and *ccr2* mRNA expression (Figure S6E,F), two genes previously described as markers for M2-like macrophages in zebrafish larvae (Nguyen-Chi et al., 2015). Altogether, these data show that PD1 has a direct impact on the kinetic of macrophage subsets recruitment by reducing the window of time during which M1-like macrophages expressing *tnfa* accumulate, presumably by promoting macrophage switch from M1-like towards M2-like phenotype. Considering that Tnfa is required for fin fold regeneration in the zebrafish (Nguyen-Chi et al., 2017), we hypothesized that its expression needs to be tightly regulated for efficient regeneration. Therefore, we tested whether increasing tnfa expression would alter regeneration in this system by injecting a recombinant zebrafish Tnfa protein at 3 h post-amputation. We showed that recombinant zebrafish Tnfa injection partially reduced regeneration of the fin fold at 48 h post-amputation, suggesting that a prolonged Tnfa impairs regeneration (Figure S7). Altogether, these data suggest that PD1 exerts a pro-regenerative potential by shortening the inflammatory phase of the regeneration process.

3.4 | PD1 inhibits macrophage activation in mouse macrophages

Since Tnfa signal is essential to prime the regeneration process (Nguyen-Chi et al., 2017) and that *tnfa* increased expression (Miskolci et al., 2019) induces regeneration defects, we hypothesized and showed above that PD1 exerts a pro-regenerative potential in zebrafish by speeding up the decrease of M1-like macrophages expressing *tnfa* frequency at the amputation site. To extend our research to mammalian systems and define at the cellular level the role of PD1, we used mouse M1-like macrophages producing TNFα generated in culture by the presence of **LPS** (Beutler & Rietschel, 2003; Medzhitov & Janeway, 2000). Unstimulated or LPS-

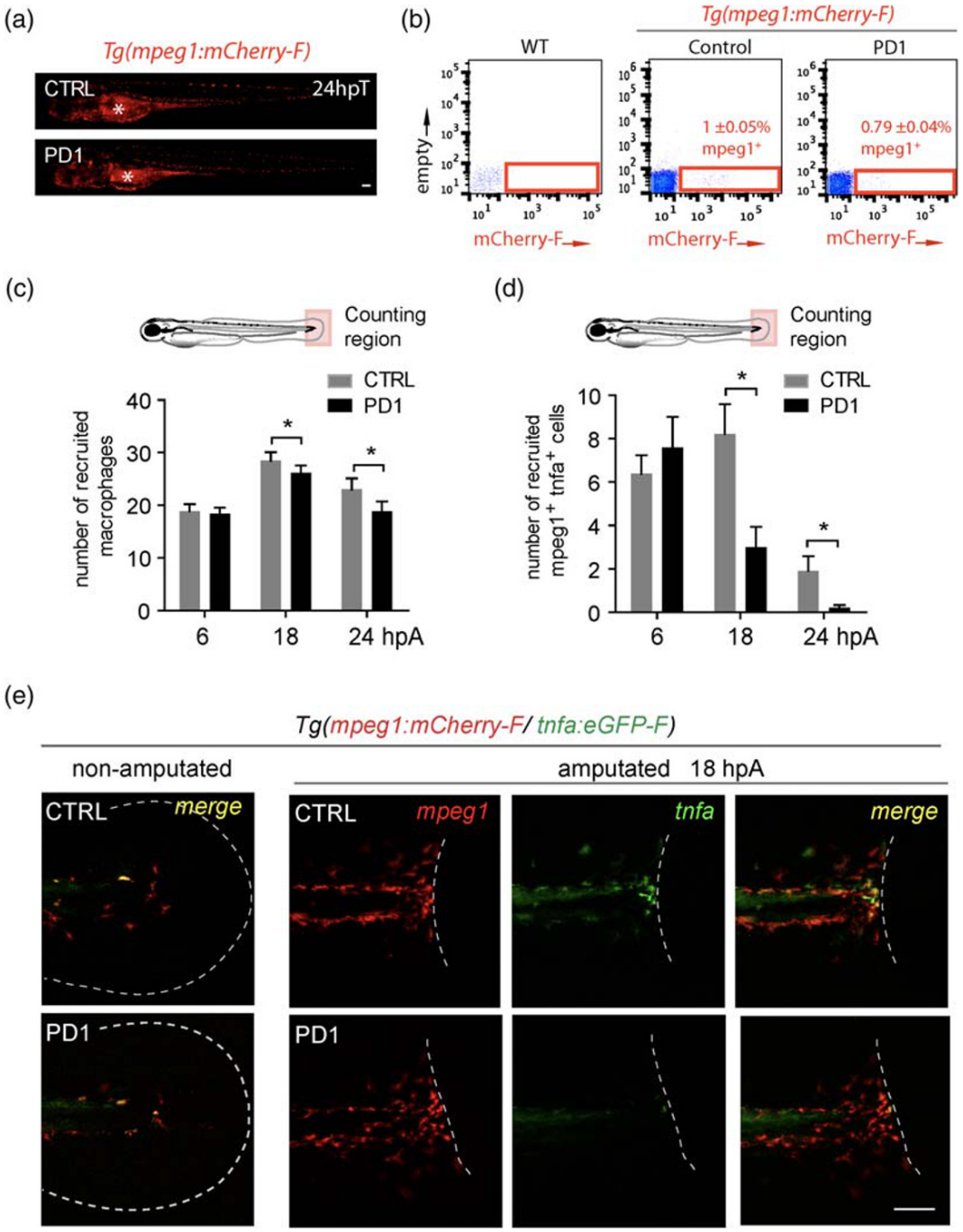

FIGURE 4 PD1 does not affect initial activation of macrophages but favours macrophage skewing towards non-inflammatory phenotypes in zebrafish. (a) *Tg(mpeg1:mCherry-F)* larvae were incubated in ethanol or in 10 μM of PD1 at 3 days post-fertilization (dpf) and mCherry fluorescence was analysed by microscopy at 0, 6 and 24 hpT. Representative images of macrophages (mCherry) in whole larvae at 24 hpT. Asterisks show the auto-fluorescence of the yolk. (b) Quantification of macrophage steady state in WT and *Tg(mpeg1:mCherry-F)* larvae 6 h after treatment with ethanol (control; CTRL) or PD1 using fluorescence-activated flow cytometry analysis of mpeg1$^+$ cells. Cells from pools of 20 larvae were collected. Gate represents mCherry-F$^+$ population (the percentage among total cells is indicated, three experiments). (c–e) *Tg(mpeg1:mCherry-F/tnfa:eGFP-F)* larvae were either kept intact or amputated at 3 dpf and then incubated with ethanol or PD1 (10 μM). The number of macrophages (mpeg1$^+$ cells) (c) and the number of activated macrophages (mpeg1$^+$ tnfa$^+$ cells) (d) that were recruited to the wound were analysed by fluorescence microscopy at different time points after wounding (mean ± SEM, for macrophage count: $n_{CTRL/6hpA}$ = 19, $n_{CTRL/18hpA}$ = 26, $n_{CTRL/24hpA}$ = 16, $n_{PD1/6hpA}$ = 22, $n_{PD1/18hpA}$ = 25, $n_{PD1/24hpA}$ = 20, from three independent experiments, Student's *t*-test, one-tailed; for activated macrophage count: $n_{CTRL/6hpA}$ = 8, $n_{CTRL/18hpA}$ = 9, $n_{CTRL/24hpA}$ = 10, $n_{PD1/6hpA}$ = 10, $n_{PD1/18hpA}$ = 8, $n_{PD1/24hpA}$ = 10, representative of two independent experiments, Mann–Whitney test, one-tailed, $^*P < 0.05$). Diagrams show the region of counting. (e) Representative fin fold images show single fluorescence channels and overlay of fluorescence channels (merge) in CTRL and PD1-treated larvae without amputation and at 18 hpA. Scale bars: 100 μm; hpA, hours post-amputation

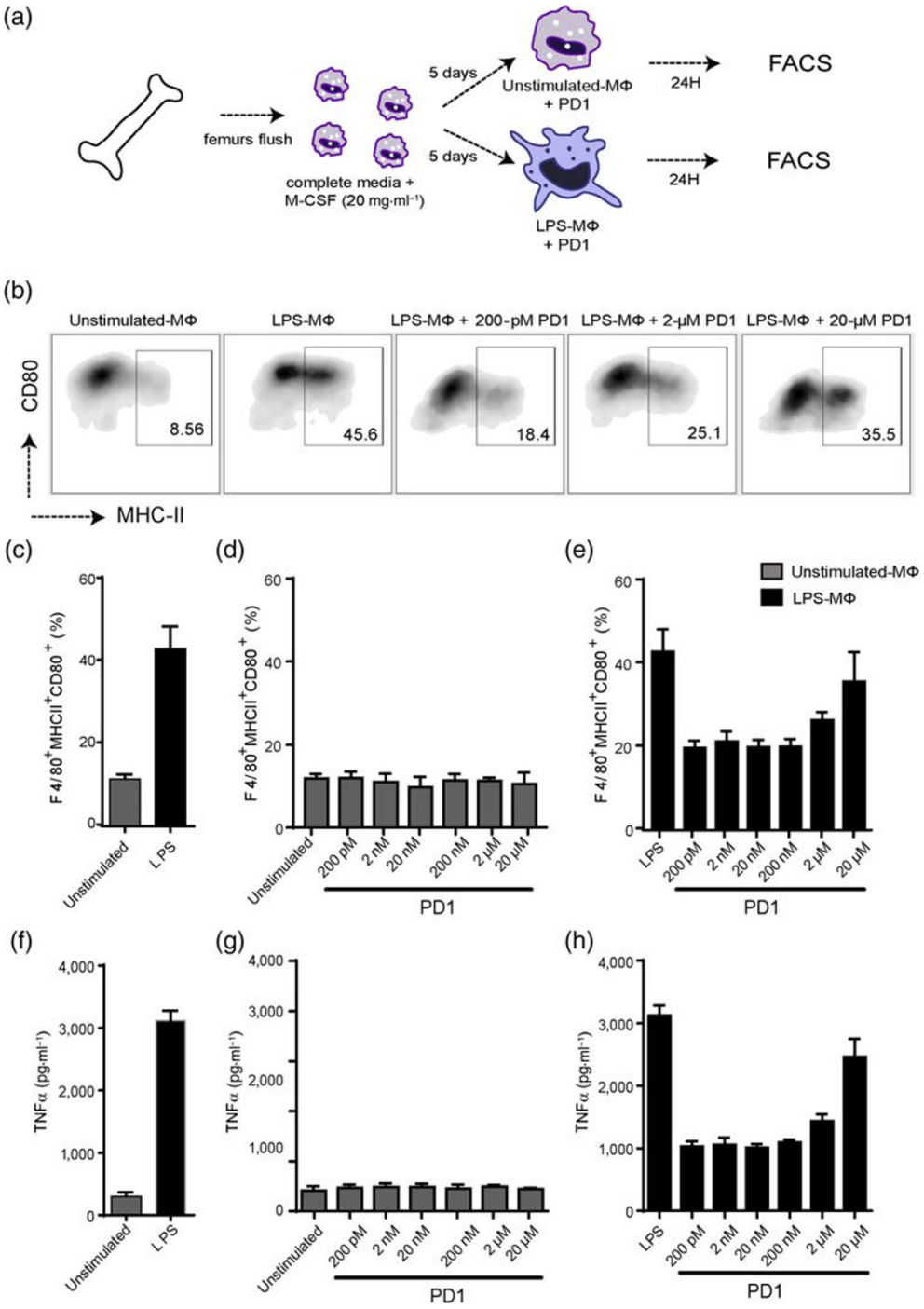

FIGURE 5 PD1 prevents LPS-induced murine macrophage stimulation. (a) Schedule of the experiment of macrophage activation with LPS. (b) Representative flow cytometry dot plot graphs showing the percentage of MHCII and CD80 positive cells among the unstimulated macrophages (Unstimulated-Mφ) and macrophages stimulated with LPS for 24 h (LPS-Mφ). PD1 was added at the same time as LPS at different concentrations (200 pM, 2 nM, 20 nM, 200 nM, 2 μM or 20 μM). (c–e) FACS quantification of the percentage of macrophages positive for F4/80, MHCII and CD80. (f,h) TNF-α quantification in the culture media of unstimulated-Mφ and LPS-Mφ cultured with six different concentrations of PD1 by ELISA (*N* = 4)

stimulated murine macrophages were cultured for 24 h without or with PD1 at six different concentrations including 200 pM, 2 nM, 20 nM, 200 nM, 2 μM and 20 μM (Figure 5a). The expression profile of macrophage activation markers including MHCII and CD80 on the surface of M1-like macrophages and their capacity to produce TNFα was assessed by FACS and ELISA respectively. After LPS stimulation, the frequency of activated M1-like macrophages positives for F4/80, CD80 and MHC-II increased as well as their capacity to produce TNFα as compared to unstimulated macrophages (Figure 5b,c,f). The addition of PD1 did not modify the percentage of $F4/80^{+}CD80^{+}MHCII^{+}$ unstimulated macrophages as well as their capacity to produce TNFα (Figure 5d,g). In contrast, PD1 addition in LPS-stimulated murine macrophages lowered the percentage of $MHCII^{+}CD80^{+}$ cells among the $F4/80^{+}$ cells as well as TNFα release (Figure 5e,h). Of note, the maximal suppressive effect of PD1 on macrophage activation was observed at a concentration of 200 pM. This effect plateaued as the dose increased until it was lost at a concentration of 20mM (Figure 5e). The decreased percentage of LPS-stimulated macrophages $MHCII^{+}CD80^{+}$ was associated with a reduced capacity of these macrophages to produce TNFα upon PD1 treatment (Figure 5h). These

preliminary results suggest that PD1 treatment reduces the activation of murine macrophages and the generation of an inflammatory environment. These data support the similarities between non-mammalian and mammalian macrophage systems in response to PD1 stimulation.

3.5 | Pro-regenerative effect of PD1 is dependent on macrophages but not neutrophils

To test whether neutrophils are important in mediating enhanced regeneration on exposure to PD1, we suppressed neutrophil population in zebrafish larvae in the presence or not of PD1 by using *Tg(mpx:gal4/UAS:nfsB-mCherry)* larvae, in which mpx promoter drives indirectly the expression of *nfsB* specifically in neutrophils. nfsB encodes an *E. coli* nitroreductase (NTR) that converts the prodrug MTZ into a toxic agent, leading to death of the expressing cells (Davison et al., 2007). *Tg(mpx:gal4/UAS:nfsB-mCherry)* larvae were treated at 48 h post-fertilization with 10-mM MTZ to deplete neutrophils (Figure 6a,b). DMSO treatment on transgenic larvae and MTZ treatment on WT siblings were used as controls. We showed that MTZ in transgenics efficiently reduced the number of neutrophils (Figure S8A,B,D) and prevented their recruitment as soon as 24 hpT (Figure S8C). Furthermore, depleted larvae were injected either with PD1 or ethanol at 3 days post-fertilization 1 h before amputation (Figure 6a,b). We observed that PD1 enhanced regeneration of the fin fold at 48 h post-amputation (hpA) regardless the presence or not of neutrophils as revealed by the regenerative fin fold length (Figure 6c) and the regenerative area (Figure 6d).

We then turned our attention to the role played by macrophages in mediating pro-regenerative effect of PD1. We suppressed macrophage population in zebrafish larvae in the presence or not of PD1 using *Tg(mpeg1:gal4/UAS:nfsB-mCherry)* larvae, in which NTR is expressed only in macrophages. We showed that MTZ treatment at 48 h post-fertilization in transgenics efficiently reduced the number of macrophages (Figure S9). Furthermore, depleted larvae were injected either with PD1 or with ethanol at 3 days post-fertilization 1 h before amputation and analysed for regeneration at 48 h post-amputation (Figure 7a, b). We observed that PD1 enhanced regeneration of the fin fold at 48 h

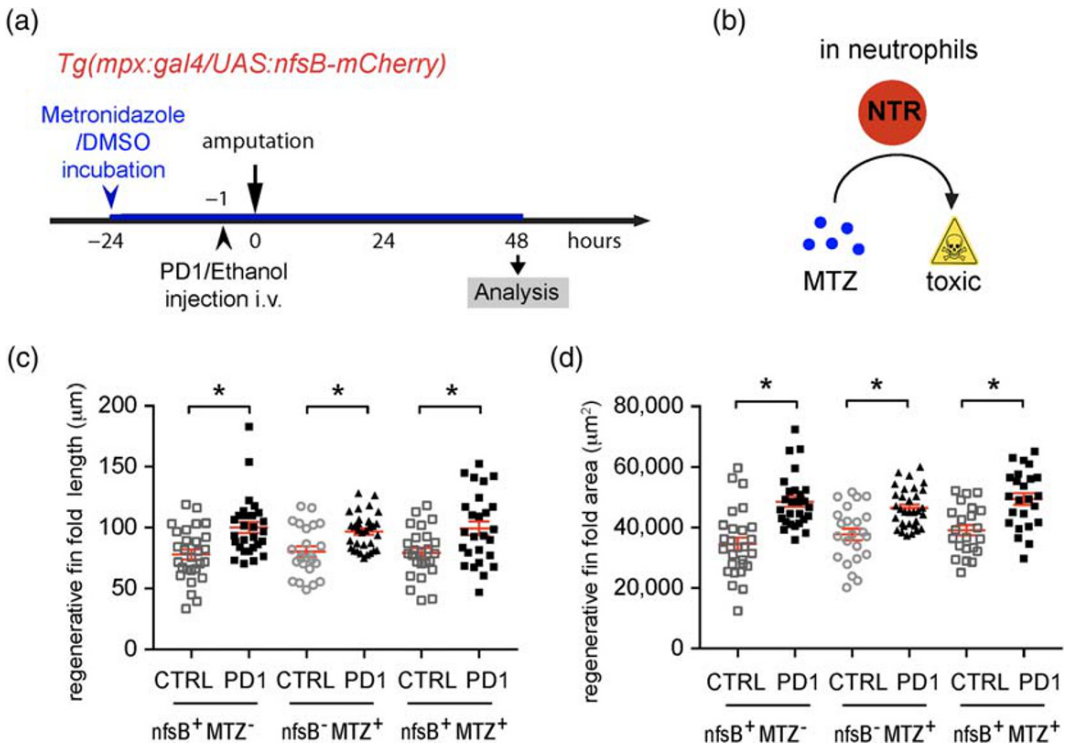

FIGURE 6 PD1 pro-regenerative effect is independent on neutrophils. (a) Schedule of the experiment of neutrophil depletion. *Tg(mpx:GAL4/UAS:nfsB-mCherry)* larvae were treated with metronidazole (*nfsB*$^{+}$ MTZ^{+}) at 48 h post-fertilization (hpf), 24 h before amputation. DMSO treatments on the same line (*nfsB*$^{+}$ MTZ^{-}) or MTZ treatments on WT siblings (*nfsB*$^{-}$ MTZ^{+}) were used as controls . At 3 days post-fertilization (dpf), larvae were injected either with ethanol (CTRL) or PD1 (200 pg) and then amputated 1 h later. They were analysed for fin fold regeneration at 48 h post-amputation (hpA). (b) Diagram showing the mode of action of *nfsB* encoded nitroreductase enzyme in neutrophils. (c) Regenerated fin fold length at 48 hpA in indicated conditions (individual larva values, mean ± SEM, from three independent experiments, $n_{nfsB\ +\ MTZ-}$ = 28, $n_{nfsB\ -\ MTZ+/CTRL}$ = 23, $n_{nfsB\ -\ MTZ+/PD1}$ = 32, $n_{nfsB\ +\ MTZ+/CTRL}$ = 25, $n_{nfsB\ +\ MTZ+/PD1}$ = 26, Mann–Whitney test, two-tailed, CTRL vs. PD1, *$P < 0.05$). (d) Regenerated fin fold area at 48 hpA in indicated conditions (individual larva values, mean ± SEM, from two independent experiments, $n_{nfsB\ +\ MTZ-}$ = 27, $n_{nfsB\ -\ MTZ+/CTRL}$ = 23 $n_{nfsB\ -\ MTZ+/PD1}$ = 32, $n_{nfsB\ +\ MTZ+/CTRL}$ = 22, $n_{nfsB\ +\ MTZ+/PD1}$ = 24, Mann–Whitney test, two-tailed, CTRL vs. PD1, * $P < 0.05$)

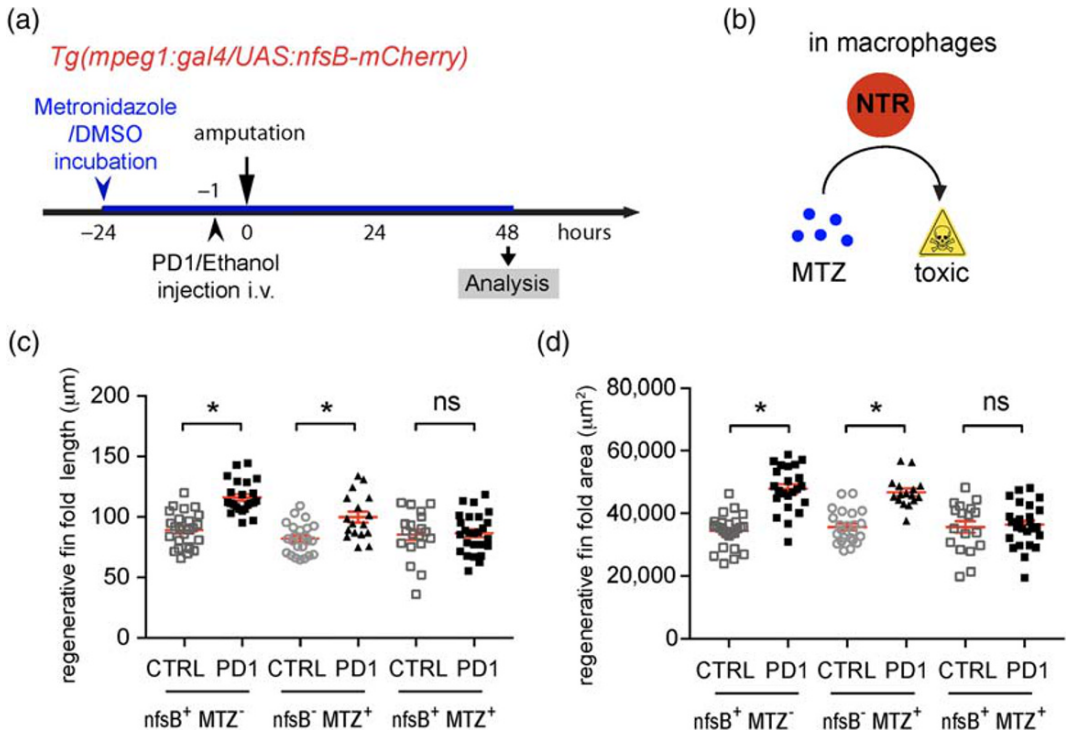

FIGURE 7 PD1 pro-regenerative effect is dependent on macrophages. (a) Schedule of the experiment of macrophage depletion. *Tg(mpeg1:GAL4/UAS:nfsB-mCherry)* larvae were treated with metronidazole (*nfsB*$^{+}$ MTZ^{+}) at 48 hpf, 24 h before amputation. DMSO treatments on the same line (*nfsB*$^{+}$ MTZ^{-}) or MTZ treatments on WT siblings (*nfsB*$^{-}$ MTZ^{+}) were used as controls . At 3 days post-fertilization (dpf), larvae were injected either with ethanol (CTRL) or PD1 (200 pg) and then amputated 1 h later. They were analysed for fin fold regeneration at 48 h post-amputation (hpA). (b) Diagram showing the mode of action of *nfsB* encoded nitroreductase enzyme in macrophages. (c) Regenerated fin fold length at 48 hpA in indicated conditions (individual larva values, mean ± SEM, from two independent experiments, $n_{nfsB\ +\ MTZ-/CTRL} = 25$, $n_{nfsB\ +\ MTZ-/PD1} = 23$, $n_{nfsB\ -\ MTZ+/CTRL} = 23$, $n_{nfsB\ -\ MTZ+/PD1} = 17$, $n_{nfsB\ +\ MTZ+/CTRL} = 19$, $n_{nfsB\ +\ MTZ+/PD1} = 26$, Student's *t*-test, two-tailed, CTRL vs. PD1, $^{*}P < 0.05$; ns, not significant). (d) Regenerated fin fold area at 48 hpA in indicated conditions (individual larva values, mean ± SEM, from two independent experiments, $n_{nfsB\ +\ MTZ-/CTRL} = 25$, $n_{nfsB\ +\ MTZ-/PD1} = 23$, $n_{nfsB\ -\ MTZ+/CTRL} = 23$, $n_{nfsB\ -\ MTZ+/PD1} = 18$, $n_{nfsB\ +\ MTZ+/CTRL} = 18$, $n_{nfsB\ +\ MTZ+/PD1} = 26$, Student's *t*-test, two-tailed, CTRL vs. PD1, $^{*}P < 0.05$; ns, non-significant)

post-amputation in the controls, while it had no effect in macrophage-depleted larvae (Figure 7c,d). To confirm this result, we suppressed macrophage population using an alternative approach. Lipo-Clodronate injection was shown to be very effective for macrophage depletion in zebrafish (Nguyen-Chi et al., 2017; Travnickova et al., 2015). Given that mpeg1 is a weak promoter and that macrophages may not be well visible at 2 days post-fertilization, we chose to switch to *Tg(mfap4:mCherry-F)* reporter line in which mfap4 promoter drives strongly and specifically the expression of a farnelylated mCherry in macrophages. We injected liposome-encapsulated clodronate (L-clodronate) in the caudal vein of 48 h post-fertilization *Tg(mfap4:mCherry-F/mpx:eGFP)* larvae, in which both macrophages and neutrophils are labelled. Liposome-encapsulated PBS (L-PBS) was used as a control. As previously reported (Travnickova et al., 2015), L-clodronate efficiently decreased macrophage number at 24 hpT, without affecting neutrophils (Figure S10). Macrophage-depleted larvae were then injected either with PD1 or ethanol at 3 days post-fertilization, 1 h before amputation (Figure 8a). While PD1 enhanced the regeneration of fin folds in L-PBS condition, it did not improve regeneration in L-clodronate condition (Figure 8b,c). In conclusion, these data showed that the pro-regenerative function of PD1 is dependent on macrophage but not neutrophils.

4 | DISCUSSION AND CONCLUSIONS

Regeneration is fundamentally important to rebuild injured organs and restore their function. Considerable attention has been given to describe cellular and molecular mechanisms involved in epimorphic regeneration in regenerative vertebrates. However, molecules that effectively stimulate regeneration are still scarce. In this study, we investigated the impact of a specialized pro-resolving mediator (SPM) on epimorphic regeneration in live vertebrates. By exposing the zebrafish larva to protectin D1 (PD1), we showed that regeneration of the caudal fin fold was effectively enhanced. This phenomenon was characterized by an increase of blastemal cell proliferation at the stump and accelerated reorganization of mesenchymal cells followed by an accelerated growth of the regenerative tissue.

Previous reports argue that some class of SPM, including PD1, carry potent protective properties and favour tissue repair. Indeed,

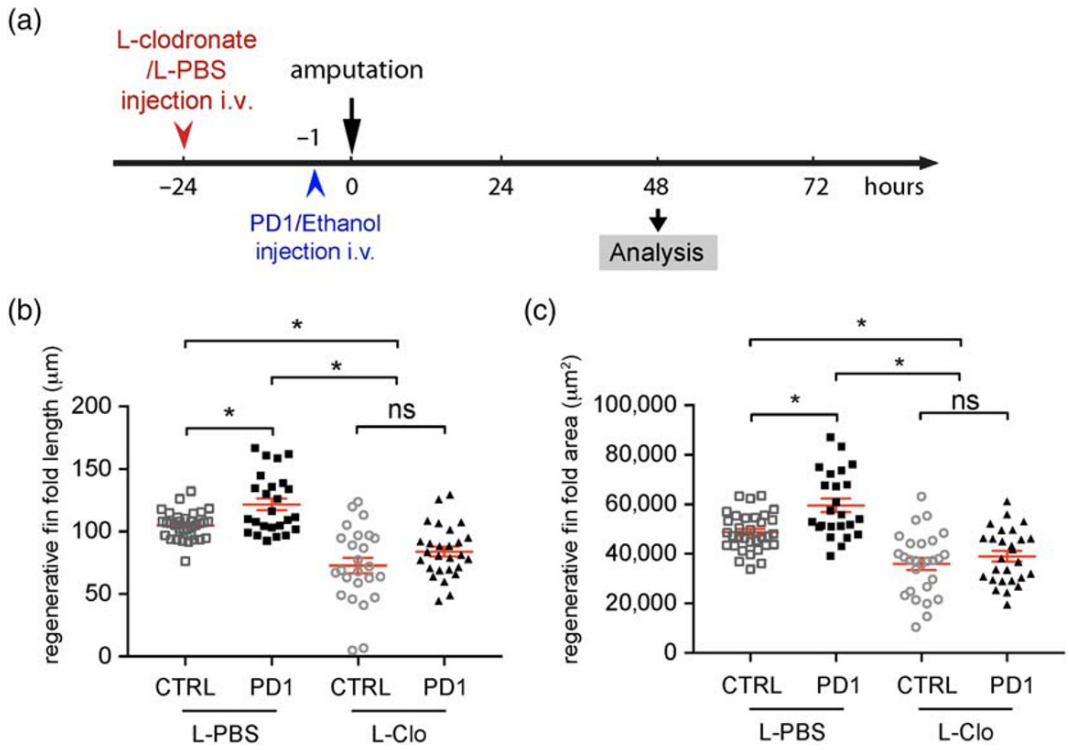

FIGURE 8 Liposome-clodronate confirms the role of macrophages in PD1 mediated-regeneration. (a) Schedule of the experiment. Macrophages were ablated using Liposome-clodronate (L-clodronate) injection in the caudal vein at 48 hpf, 24 h before amputation. Lipo-PBS injection was used as a control . At 3 days post-fertilization , larvae were injected either with ethanol (CTRL) or with PD1 (200 pg) and then amputated 1 h later. Caudal fin regeneration was analysed at 48 hpA by microscopy. (b) Regenerated fin length at 48 hpA in indicated conditions (individual larva values, mean ± SEM, from two independent experiments, $n_{PBS/CTRL}$ = 34, $n_{PBS/PD1}$ = 25, $n_{clo/CTRL}$ = 25, $n_{clo/PD1}$ = 27, ANOVA, Tukey's post-hoc test, *P < 0.05). (c) Regenerated fin area at 48 hpA in indicated conditions (individual larva values, mean ± SEM, from two independent experiments, $n_{PBS/CTRL}$ = 33, $n_{PBS/PD1}$ = 24, $n_{clo/CTRL}$ = 27, $n_{clo/PD1}$ = 27, ANOVA, Tukey's post-hoc test, *P < 0.05)

PD1 accelerates healing and nerve-fibre growth of skin wounds of diabetic mice (Hong et al., 2014). Similar protective effects were observed on mouse wound model with **resolvin D2** (Bohr et al., 2013) and the peptide **chemerin** 15 (Cash et al., 2014). Similarly, D-series resolvins which are produced by the wound during skin injury in mice and pigs were shown to direct a receptor-mediated role in the normal tissue repair programme (Hellmann et al., 2018). Recently, a mediator lipidome mapping revealed dynamic lipid mediator changes within macrophages subtypes during muscle regeneration in mouse supporting a role for SPM in macrophage phenotype transition and muscle regeneration (Giannakis et al., 2019). Moreover, PD1-related SPMs, maresin 1 and two sulfido-conjugate mediators (13-glutathionyl, 14-hydroxy-DHA and 13-cysteinylglycinyl, 14-hydroxy-DHA) were shown to carry pro-regenerative role in planarian species (Dalli et al., 2016; Dalli, Chiang, & Serhan, 2014; Serhan et al., 2012). Although these SPMs accelerate epimorphic regeneration in planarian after surgical injury, it remains to be determined whether SPMs activate similar mechanisms as in vertebrates, that is, activation of blastema formation or control of equivalent immune cells.

The pro-regenerative activity of PD1 relies presumably on its ability to shorten the inflammation phase and accelerate inflammation resolution. In this study, we provided evidence that PD1 acts at least in two ways, (1) it reduces neutrophil presence at the wound through an unexpected mechanism, the reverse migration of these cells and (2) it favours macrophage phenotype switch from a pro-inflammatory to a non-inflammatory state. PD1 most likely achieves its pro-regenerative effect through the direct control of macrophage function since specific suppression of macrophages but not neutrophils prevents enhanced regeneration on exposure to PD1. Human neutrophil reverse migration was previously shown to be induced by the SPM lipoxins (Hamza et al., 2014), suggesting that lipoxins and protectins may share the property to drive retrotaxis of neutrophils. This reverse migration may be a consequence of macrophage phenotype switch, as macrophage was shown to drive neutrophil removal through the production of **PGE_2** (Loynes et al., 2018). These findings are in agreement with studies from others and our group that report the essential role of macrophage in appendage regeneration in vertebrates (Godwin et al., 2013; Hasegawa et al., 2017; Nguyen-Chi et al., 2017; Petrie et al., 2014). In these systems, the exquisite regulation of macrophage states seems pivotal to determine the wound fate since deletion of pro-inflammatory macrophages or regenerative phase-associated macrophages both lead to impaired regeneration. It is important to note that neither initial neutrophil recruitment nor macrophage activation are affected by PD1 exposure. Since pro-inflammatory signals like Tnfa and Il1b are essential to prime regeneration (Hasegawa et al., 2017; Nguyen-Chi et al., 2017; Tsarouchas et al., 2018) and that

an increase of tnfa expression (this study and Miskolci et al., 2019) leads to regeneration defects, we propose that PD1 exerts a pro-regenerative potential by speeding up the resolution phase without affecting the onset of inflammation.

In addition, our analyses show that PD1 treatment modulates the expression of some M1-like and M2-like markers in zebrafish tails suggesting that PD1 accelerates the switch of macrophage phenotypes. Using a mammalian system, we show that PD1 also decreases M1 polarization in mouse macrophages after activation with LPS. Similarly, PD1 was recently shown to decrease expression of pro-inflammatory cytokines in LPS-activated human macrophages, presumably through a direct activation of **PPARs** genes (Bosviel et al., 2017). The conservation of PD1 function between zebrafish and mammalian systems emphasizes the relevance of the tractable zebrafish larvae system for the study of SPMs. While SPM bioactions are mediated by individual GPCRs, these receptors are, for most of them, conserved in the zebrafish. Recently, PD1 was shown to signal through **GPR37**, whose activation in murin macrophages increased phagocytosis and altered cytokine release, promoting resolution of inflammatory pain (Bang et al., 2018). Two *gpr37* exist in zebrafish, *gpr37a* and *gpr37b*, whether PD1 binds to Gpr37 proteins or to other receptors in zebrafish still needs to be investigated. Finally, our data add to the increasingly diverse roles of SPMs and support the potential of PD1 and related molecules as a therapeutic for inflammatory and degenerative disorders.

ACKNOWLEDGEMENTS

We thank the imaging facility MRI, member of the national infrastructure France-BioImaging infrastructure supported by the French National Research Agency (ANR-10-INBS-04, "Investments for the future"), Laure Yatime for the analysis of GPR37 orthologues in the zebrafish, J-P. Levraud (Institut Pasteur, France) for trans-shipping the *Tg(mpx:Dendra2)uwm4* line, *Tg(mpeg1:Gal4/UAS:nfsB-mCherry)* line and *Tg(mpx:Gal4/UAS:nfsB-mCherry)* and M. Bagnat for *Tg(rcn3:gal4/UAS:mCherry)* line. We also thank Catherine Gonzalez and Stephane Castel for taking care of the Zebrafish facility of the University of Montpellier. We thank Victor Mulero for sending the recombinant zfTnfa. This work was supported by INSERM, a grant from the European Community's H2020 Program (Marie-Curie Innovative Training Network ImageInLife: Grant Agreement no. 721537). Funding sources had no role in the writing of the manuscript or the decision to submit it for publication. The corresponding author had full access to all the data in the study and had final responsibility for the decision to submit for publication.

AUTHOR CONTRIBUTIONS

M.N.C. and P.L.C. designed experiments with input from L.B., G.L., T.D., C.J. and F.D. M.N.C., P.L.C., L.B., T.S., A.B. and R.C. performed experiments. M.N.C. and F.D. wrote the manuscript with input from G.L., T.D., T.S., L.B. and C.J.

CONFLICT OF INTEREST

The authors have no conflicts of interest to declare.

DECLARATION OF TRANSPARENCY AND SCIENTIFIC RIGOUR

This declaration acknowledges that this paper adheres to the principles for transparent reporting and scientific rigour of preclinical research as stated in the BJP guidelines for Design and Analysis, Immunoblotting and Immunochemistry and Animal Experimentation, and as recommended by funding agencies, publishers and other organisations engaged with supporting research.

ORCID

Mai Nguyen-Chi https://orcid.org/0000-0003-2672-2426

REFERENCES

Akimenko, M.-A., Marí-Beffa, M., Becerra, J., & Géraudie, J. (2003). Old questions, new tools, and some answers to the mystery of fin regeneration: Fin Regeneration. *Developmental Dynamics*, *226*, 190–201. https://doi.org/10.1002/dvdy.10248

Alexander, S. P. H., Christopoulos, A., Davenport, A. P., Kelly, E., Mathie, A., Peters, J. A., … CGTP Collaborators. (2019). THE CONCISE GUIDE TO PHARMACOLOGY 2019/20: G protein-coupled receptors. *British Journal of Pharmacology*, *176*(Suppl 1), S21–S141.

Alexander, S. P. H., Roberts, R. E., Broughton, B. R. S., Sobey, C. G., George, C. H., Stanford, S. C., … Ahluwalia, A. (2018). Goals and practicalities of immunoblotting and immunohistochemistry: A guide for submission to the British Journal of Pharmacology: Editorial. *British Journal of Pharmacology*, *175*, 407–411. https://doi.org/10.1111/bph.14112

Alvarado, A. S., & Tsonis, P. A. (2006). Bridging the regeneration gap: Genetic insights from diverse animal models. *Nature Reviews Genetics*, *7*, 873–884. https://doi.org/10.1038/nrg1923

Balas, L., & Durand, T. (2016). Dihydroxylated E,E,Z-docosatrienes. An overview of their synthesis and biological significance. *Progress in Lipid Research*, *61*, 1–18. https://doi.org/10.1016/j.plipres.2015.10.002

Balas, L., Guichardant, M., Durand, T., & Lagarde, M. (2014). Confusion between protectin D1 (PD1) and its isomer protectin DX (PDX). An overview on the dihydroxy-docosatrienes described to date. *Biochimie*, *99*, 1–7. https://doi.org/10.1016/j.biochi.2013.11.006

Bang, S., Xie, Y.-K., Zhang, Z.-J., Wang, Z., Xu, Z.-Z., & Ji, R.-R. (2018). GPR37 regulates macrophage phagocytosis and resolution of inflammatory pain. *Journal of Clinical Investigation*, *128*, 3568–3582. https://doi.org/10.1172/JCI99888

Bannenberg, G. L., Chiang, N., Ariel, A., Arita, M., Tjonahen, E., Gotlinger, K. H., … Serhan, C. N. (2005). Molecular circuits of resolution: Formation and actions of resolvins and protectins. *Journal of Immunology*, *174*, 4345–4355. https://doi.org/10.4049/jimmunol.174.7.4345

Beutler, B., & Rietschel, E. T. (2003). Innate immune sensing and its roots: The story of endotoxin. *Nature Reviews. Immunology*, *3*, 169–176. https://doi.org/10.1038/nri1004

Bohr, S., Patel, S. J., Sarin, D., Irimia, D., Yarmush, M. L., & Berthiaume, F. (2013). Resolvin D2 prevents secondary thrombosis and necrosis in a mouse burn wound model: RvD2 prevents secondary necrosis in burns. *Wound Repair and Regeneration*, *21*, 35–43. https://doi.org/10.1111/j.1524-475X.2012.00853.x

Bosviel, R., Joumard-Cubizolles, L., Chinetti-Gbaguidi, G., Bayle, D., Copin, C., Hennuyer, N., … Gladine, C. (2017). DHA-derived oxylipins, neuroprostanes and protectins, differentially and dose-dependently modulate the inflammatory response in human macrophages: Putative mechanisms through PPAR activation. *Free Radical Biology and Medicine*, *103*, 146–154. https://doi.org/10.1016/j.freeradbiomed.2016.12.018

Cash, J. L., Bass, M. D., Campbell, J., Barnes, M., Kubes, P., & Martin, P. (2014). Resolution mediator Chemerin15 reprograms the wound microenvironment to promote repair and reduce scarring. *Current Biology*, *24*, 1406–1414. https://doi.org/10.1016/j.cub.2014.05.006

Chiang, N., Fredman, G., Bäckhed, F., Oh, S. F., Vickery, T., Schmidt, B. A., & Serhan, C. N. (2012). Infection regulates pro-resolving mediators that lower antibiotic requirements. *Nature*, *484*, 524–528. https://doi.org/10.1038/nature11042

Curtis, M. J., Alexander, S., Cirino, G., Docherty, J. R., George, C. H., Giembycz, M. A., … Ahluwalia, A. (2018). Experimental design and analysis and their reporting II: Updated and simplified guidance for authors and peer reviewers: Editorial. *British Journal of Pharmacology*, *175*, 987–993. https://doi.org/10.1111/bph.14153

Dalli, J., Chiang, N., & Serhan, C. N. (2014). Identification of 14-series sulfido-conjugated mediators that promote resolution of infection and organ protection. *Proceedings of the National Academy of Sciences*, *111*, E4753–E4761. https://doi.org/10.1073/pnas.1415006111

Dalli, J., Colas, R. A., & Serhan, C. N. (2013). Novel n-3 immunoresolvents: Structures and actions. *Scientific Reports*, *3*, 1940. https://doi.org/10.1038/srep01940

Dalli, J., & Serhan, C. N. (2017). Pro-resolving mediators in regulating and conferring macrophage function. *Frontiers in Immunology*, *8*, 1400. https://doi.org/10.3389/fimmu.2017.01400

Dalli, J., Vlasakov, I., Riley, I. R., Rodriguez, A. R., Spur, B. W., Petasis, N. A., … Serhan, C. N. (2016). Maresin conjugates in tissue regeneration biosynthesis enzymes in human macrophages. *Proceedings of the National Academy of Sciences of the United States of America*, *113*, 12232–12237. https://doi.org/10.1073/pnas.1607003113

Dalli, J., Zhu, M., Vlasenko, N. A., Deng, B., Haeggström, J. Z., Petasis, N. A., & Serhan, C. N. (2013). The novel 13S,14S-epoxymaresin is converted by human macrophages to maresin 1 (MaR1), inhibits leukotriene A4 hydrolase (LTA4H), and shifts macrophage phenotype. *The FASEB Journal*, *27*, 2573–2583. https://doi.org/10.1096/fj.13-227728

Davison, J. M., Akitake, C. M., Goll, M. G., Rhee, J. M., Gosse, N., Baier, H., … Parsons, M. J. (2007). Transactivation from Gal4-VP16 transgenic insertions for tissue-specific cell labeling and ablation in zebrafish. *Developmental Biology*, *304*, 811–824. https://doi.org/10.1016/j.ydbio.2007.01.033

Dayaker, G., Durand, T., & Balas, L. (2014). A versatile and stereocontrolled total synthesis of dihydroxylated docosatrienes containing a conjugated *E,E,Z*-Triene. *Chemistry - A European Journal*, *20*, 2879–2887. https://doi.org/10.1002/chem.201304526

Elks, P. M., van Eeden, F. J., Dixon, G., Wang, X., Reyes-Aldasoro, C. C., Ingham, P. W., … Renshaw, S. A. (2011). Activation of hypoxia-inducible factor-1 (Hif-1) delays inflammation resolution by reducing neutrophil apoptosis and reverse migration in a zebrafish inflammation model. *Blood*, *118*, 712–722. https://doi.org/10.1182/blood-2010-12-324186

Ellett, F., Pase, L., Hayman, J. W., Andrianopoulos, A., & Lieschke, G. J. (2011). mpeg1 promoter transgenes direct macrophage-lineage expression in zebrafish. *Blood*, *117*, e49–e56. https://doi.org/10.1182/blood-2010-10-314120

Ellis, K., Bagwell, J., & Bagnat, M. (2013). Notochord vacuoles are lysosome-related organelles that function in axis and spine morphogenesis. *The Journal of Cell Biology*, *200*, 667–679. https://doi.org/10.1083/jcb.201212095

Gemberling, M., Bailey, T. J., Hyde, D. R., & Poss, K. D. (2013). The zebrafish as a model for complex tissue regeneration. *Trends in Genetics*, *29*, 611–620. https://doi.org/10.1016/j.tig.2013.07.003

Giannakis, N., Sansbury, B. E., Patsalos, A., Hays, T. T., Riley, C. O., Han, X., … Nagy, L. (2019). Dynamic changes to lipid mediators support transitions among macrophage subtypes during muscle regeneration. *Nature Immunology*, *20*, 626–636. https://doi.org/10.1038/s41590-019-0356-7

Godwin, J. W., Pinto, A. R., & Rosenthal, N. A. (2013). Macrophages are required for adult salamander limb regeneration. *Proceedings of the National Academy of Sciences*, *110*, 9415–9420. https://doi.org/10.1073/pnas.1300290110

Hall, C., Flores, M., Storm, T., Crosier, K., & Crosier, P. (2007). The zebrafish lysozyme C promoter drives myeloid-specific expression in transgenic fish. *BMC Developmental Biology*, *7*, 42. https://doi.org/10.1186/1471-213X-7-42

Hamza, B., Wong, E., Patel, S., Cho, H., Martel, J., & Irimia, D. (2014). Retrotaxis of human neutrophils during mechanical confinement inside microfluidic channels. *Integrative Biology*, *6*, 175–183. https://doi.org/10.1039/C3IB40175H

Hansen, T. V., Vik, A., & Serhan, C. N. (2019). The protectin family of specialized pro-resolving mediators: Potent immunoresolvents enabling innovative approaches to target obesity and diabetes. *Frontiers in Pharmacology*, *9*, 1582. https://doi.org/10.3389/fphar.2018.01582

Harding, S. D., Sharman, J. L., Faccenda, E., Southan, C., Pawson, A. J., Ireland, S., … NC-IUPHAR. (2018). The IUPHAR/BPS Guide to PHARMACOLOGY in 2018: Updates and expansion to encompass the new guide to IMMUNOPHARMACOLOGY. *Nucleic Acids Research*, *46*, D1091–D1106. https://doi.org/10.1093/nar/gkx1121

Hasegawa, T., Hall, C. J., Crosier, P. S., Abe, G., Kawakami, K., Kudo, A., & Kawakami, A. (2017). Transient inflammatory response mediated by interleukin-1β is required for proper regeneration in zebrafish fin fold. *eLife*, *6*, e22716.

Hellmann, J., Sansbury, B. E., Wong, B., Li, X., Singh, M., Nuutila, K., … Spite, M. (2018). Biosynthesis of D-Series resolvins in skin provides insights into their role in tissue repair. *Journal of Investigative Dermatology*, *138*, 2051–2060. https://doi.org/10.1016/j.jid.2018.03.1498

Hong, S., Lu, Y., Yang, R., Gotlinger, K. H., Petasis, N. A., & Serhan, C. N. (2007). Resolvin D1, protectin D1, and related docosahexaenoic acid-derived products: Analysis via electrospray/low energy tandem mass spectrometry based on spectra and fragmentation mechanisms. *Journal of the American Society for Mass Spectrometry*, *18*, 128–144. https://doi.org/10.1016/j.jasms.2006.09.002

Hong, S., Tian, H., Lu, Y., Laborde, J. M., Muhale, F. A., Wang, Q., … Bazan, N. G. (2014). Neuroprotectin/protectin D1: Endogenous biosynthesis and actions on diabetic macrophages in promoting wound healing and innervation impaired by diabetes. *American Journal of Physiology-Cell Physiology*, *307*, C1058–C1067. https://doi.org/10.1152/ajpcell.00270.2014

Jónasdóttir, H. S., Papan, C., Fabritz, S., Balas, L., Durand, T., Hardardottir, I., … Giera, M. (2015). Differential mobility separation of leukotrienes and protectins. *Analytical Chemistry*, *87*, 5036–5040. https://doi.org/10.1021/acs.analchem.5b00786

Kawakami, A., Fukazawa, T., & Takeda, H. (2004). Early fin primordia of zebrafish larvae regenerate by a similar growth control mechanism with adult regeneration. *Developmental Dynamics*, *231*, 693–699. https://doi.org/10.1002/dvdy.20181

Kilkenny, C., Browne, W., Cuthill, I. C., Emerson, M., & Altman, D. G. (2010). Animal research: Reporting *in vivo* experiments: the ARRIVE guidelines. *British Journal of Pharmacology*, *160*, 1577–1579.

Kimmel, C. B., Ballard, W. W., Kimmel, S. R., Ullmann, B., & Schilling, T. F. (1995). Stages of embryonic development of the zebrafish. *Developmental Dynamics*, *203*, 253–310. https://doi.org/10.1002/aja.1002030302

Larouche, J., Sheoran, S., Maruyama, K., & Martino, M. M. (2018). Immune regulation of skin wound healing: Mechanisms and novel therapeutic targets. *Advances in Wound Care*, *7*, 209–231. https://doi.org/10.1089/wound.2017.0761

Lastrucci, C., Baillif, V., Behar, A., Al Saati, T., Dubourdeau, M., Maridonneau-Parini, I., & Cougoule, C. (2015). Molecular and cellular profiles of the resolution phase in a damage-associated molecular pattern (DAMP)-mediated peritonitis model and revelation of leukocyte

persistence in peritoneal tissues. *The FASEB Journal*, *29*, 1914–1929. https://doi.org/10.1096/fj.14-259341

Loynes, C. A., Lee, J. A., Robertson, A. L., Steel, M. J. G., Ellett, F., Feng, Y., … Renshaw, S. A. (2018). PGE2 production at sites of tissue injury promotes an anti-inflammatory neutrophil phenotype and determines the outcome of inflammation resolution in vivo. *Science Advances*, *4*, eaar8320. https://advances.sciencemag.org/content/4/9/eaar8320

Mateus, R., Pereira, T., Sousa, S., de Lima, J. E., Pascoal, S., Saúde, L., & Jacinto, A. (2012). In vivo cell and tissue dynamics underlying zebrafish fin fold regeneration. *PLoS ONE*, *7*, e51766. https://doi.org/10.1371/journal.pone.0051766

Mathew, L. K., Sengupta, S., Kawakami, A., Andreasen, E. A., Löhr, C. V., Loynes, C. A., … Tanguay, R. L. (2007). Unraveling tissue regeneration pathways using chemical genetics. *The Journal of Biological Chemistry*, *282*, 35202–35210. https://doi.org/10.1074/jbc.M706640200

Mathias, J. R., Perrin, B. J., Liu, T.-X., Kanki, J., Look, A. T., & Huttenlocher, A. (2006). Resolution of inflammation by retrograde chemotaxis of neutrophils in transgenic zebrafish. *Journal of Leukocyte Biology*, *80*, 1281–1288. https://doi.org/10.1189/jlb.0506346

Medzhitov, R., & Janeway, C. (2000). Innate immune recognition: Mechanisms and pathways. *Immunological Reviews*, *173*, 89–97. https://doi.org/10.1034/j.1600-065X.2000.917309.x

Mescher, A. L., Neff, A. W., & King, M. W. (2017). Inflammation and immunity in organ regeneration. *Developmental & Comparative Immunology*, *66*, 98–110. https://doi.org/10.1016/j.dci.2016.02.015

Miskolci, V., Squirrell, J., Rindy, J., Vincent, W., Sauer, J. D., Gibson, A., … Huttenlocher, A. (2019). Distinct inflammatory and wound healing responses to complex caudal fin injuries of larval zebrafish. *eLife*, *8*, e45976. https://doi.org/10.7554/eLife.45976

Nguyen-Chi, M., Laplace-Builhé, B., Travnickova, J., Luz-Crawford, P., Tejedor, G., Lutfalla, G., … Djouad, F. (2017). TNF signaling and macrophages govern fin regeneration in zebrafish larvae. *Cell Death & Disease*, *8*, e2979. https://doi.org/10.1038/cddis.2017.374

Nguyen-Chi, M., Laplace-Builhe, B., Travnickova, J., Luz-Crawford, P., Tejedor, G., Phan, Q. T., … Djouad, F. (2015). Identification of polarized macrophage subsets in zebrafish. *eLife*, *4*, e07288. https://doi.org/10.7554/eLife.07288

Nguyen-Chi, M., Phan, Q. T., Gonzalez, C., Dubremetz, J.-F., Levraud, J.-P., & Lutfalla, G. (2014). Transient infection of the zebrafish notochord with E. coli induces chronic inflammation. *Disease Models & Mechanisms*, *7*, 871–882. https://doi.org/10.1242/dmm.014498

Nguyen-Chi, M. E., Bryson-Richardson, R., Sonntag, C., Hall, T. E., Gibson, A., Sztal, T., … Currie, P. D. (2012). Morphogenesis and cell fate determination within the adaxial cell equivalence group of the zebrafish myotome. *PLoS Genetics*, *8*, e1003014. https://doi.org/10.1371/journal.pgen.1003014

Nourshargh, S., Renshaw, S. A., & Imhof, B. A. (2016). Reverse migration of neutrophils: Where, when, how, and why? *Trends in Immunology*, *37*, 273–286. https://doi.org/10.1016/j.it.2016.03.006

Petasis, N. A., Yang, R., Winkler, J. W., Zhu, M., Uddin, J., Bazan, N. G., & Serhan, C. N. (2012). Stereocontrolled total synthesis of neuroprotectin D1/Protectin D1 and its aspirin-triggered stereoisomer. *Tetrahedron Letters*, *53*, 1695–1698. https://doi.org/10.1016/j.tetlet.2012.01.032

Petrie, T. A., Strand, N. S., Tsung-Yang, C., Rabinowitz, J. S., & Moon, R. T. (2014). Macrophages modulate adult zebrafish tail fin regeneration. *Development*, *141*, 2581–2591. https://doi.org/10.1242/dev.098459

Phan, Q. T., Sipka, T., Gonzalez, C., Levraud, J.-P., Lutfalla, G., & Nguyen-Chi, M. (2018). Neutrophils use superoxide to control bacterial infection at a distance. *PLoS Pathogens*, *14*, e1007157. https://doi.org/10.1371/journal.ppat.1007157

Pistorius, K., Souza, P. R., De Matteis, R., Austin-Williams, S., Primdahl, K. G., Vik, A., … Dalli, J. (2018). PDn-3 DPA pathway regulates human monocyte differentiation and macrophage function. *Cell Chemical Biology*, *25*, 749–760.e9. https://doi.org/10.1016/j.chembiol.2018.04.017

Ramon, S., Dalli, J., Sanger, J. M., Winkler, J. W., Aursnes, M., Tungen, J. E., … Serhan, C. N. (2016). The protectin PCTR1 is produced by human M2 macrophages and enhances resolution of infectious inflammation. *The American Journal of Pathology*, *186*, 962–973. https://doi.org/10.1016/j.ajpath.2015.12.012

Renshaw, S. A., Loynes, C. A., Trushell, D. M. I., Elworthy, S., Ingham, P. W., & Whyte, M. K. B. (2006). A transgenic zebrafish model of neutrophilic inflammation. *Blood*, *108*, 3976–3978. https://doi.org/10.1182/blood-2006-05-024075

Robertson, A. L., Holmes, G. R., Bojarczuk, A. N., Burgon, J., Loynes, C. A., Chimen, M., … Renshaw, S. A. (2014). A zebrafish compound screen reveals modulation of neutrophil reverse migration as an anti-inflammatory mechanism. *Science Translational Medicine*, *6*, 225ra29–225ra29. https://doi.org/10.1126/scitranslmed.3007672

Roca, F. J., Mulero, I., López-Muñoz, A., Sepulcre, M. P., Renshaw, S. A., Meseguer, J., & Mulero, V. (2008). Evolution of the inflammatory response in vertebrates: Fish TNF-α is a powerful activator of endothelial cells but hardly activates phagocytes. *Journal of Immunology*, *181*, 5071–5081. https://doi.org/10.4049/jimmunol.181.7.5071

Serhan, C. N. (2014). Pro-resolving lipid mediators are leads for resolution physiology. *Nature*, *510*, 92–101. https://doi.org/10.1038/nature13479

Serhan, C. N., Chiang, N., & Dalli, J. (2015). The resolution code of acute inflammation: Novel pro-resolving lipid mediators in resolution. *Seminars in Immunology*, *27*, 200–215. https://doi.org/10.1016/j.smim.2015.03.004

Serhan, C. N., Dalli, J., Karamnov, S., Choi, A., Park, C.-K., Xu, Z.-Z., … Petasis, N. A. (2012). Macrophage proresolving mediator maresin 1 stimulates tissue regeneration and controls pain. *The FASEB Journal*, *26*, 1755–1765. https://doi.org/10.1096/fj.11-201442

Serhan, C. N., Gotlinger, K., Hong, S., Lu, Y., Siegelman, J., Baer, T., … Petasis, N. A. (2006). Anti-inflammatory actions of neuroprotectin D1/protectin D1 and its natural stereoisomers: Assignments of dihydroxy-containing docosatrienes. *Journal of Immunology*, *176*, 1848–1859. https://doi.org/10.4049/jimmunol.176.3.1848

Simkin, J., Gawriluk, T. R., Gensel, J. C., & Seifert, A. W. (2017). Macrophages are necessary for epimorphic regeneration in African spiny mice. *eLife*, *6*, e24623. https://doi.org/10.7554/eLife.24623

Spite, M., Clària, J., & Serhan, C. N. (2014). Resolvins, specialized proresolving lipid mediators, and their potential roles in metabolic diseases. *Cell Metabolism*, *19*, 21–36. https://doi.org/10.1016/j.cmet.2013.10.006

Tal, T. L., Franzosa, J. A., & Tanguay, R. L. (2010). Molecular signaling networks that choreograph epimorphic fin regeneration in zebrafish—A mini-review. *Gerontology*, *56*, 231–240. https://doi.org/10.1159/000259327

Tharp, W. G., Yadav, R., Irimia, D., Upadhyaya, A., Samadani, A., Hurtado, O., … Poznansky, M. C. (2006). Neutrophil chemorepulsion in defined interleukin-8 gradients in vitro and in vivo. *Journal of Leukocyte Biology*, *79*, 539–554. https://doi.org/10.1189/jlb.0905516

Travnickova, J., Tran Chau, V., Julien, E., Mateos-Langerak, J., Gonzalez, C., Lelièvre, E., … Kissa, K. (2015). Primitive macrophages control HSPC mobilization and definitive haematopoiesis. *Nature Communications*, *6*, 6227. https://doi.org/10.1038/ncomms7227

Tsarouchas, T. M., Wehner, D., Cavone, L., Munir, T., Keatinge, M., Lambertus, M., … Becker, C. G. (2018). Dynamic control of proinflammatory cytokines Il-1β and Tnf-α by macrophages in zebrafish spinal cord regeneration. *Nature Communications*, *9*, 4670. https://doi.org/10.1038/s41467-018-07036-w

Xu, Z.-Z., Liu, X.-J., Berta, T., Park, C.-K., Lü, N., Serhan, C. N., & Ji, R.-R. (2013). Neuroprotectin/protectin D1 protects against neuropathic pain in mice after nerve trauma: NPD1/PD1 and neuropathic pain. *Annals of Neurology*, *74*, 490–495. https://doi.org/10.1002/ana.23928

Yoo, S. K., & Huttenlocher, A. (2011). Spatiotemporal photolabeling of neutrophil trafficking during inflammation in live zebrafish. *Journal of Leukocyte Biology*, *89*, 661–667. https://doi.org/10.1189/jlb.1010567

SUPPORTING INFORMATION

Additional supporting information may be found online in the Supporting Information section at the end of this article.